News from the CTEQ-TEA group

Pavel Nadolsky (Southern Methodist University, USA)

With the CTEQ-TEA (Tung Et. Al.) working group

China: A. Ablat, S. Dulat, Y. Fu, T.-J. Hou, I. Sitiwaldi

Mexico: A. Courtoy

USA: M. Guzzi., P. N., T.J. Hobbs, J. Huston, H.-W. Lin, C. Schmidt, K. Xie, C.-P. Yuan

and other coauthors

Reviews of recent results in 2408.04020 (accepted by EPJP) and 2408.11131; see also talks by Courtoy, Guzzi, Mohan

• RESEARCH PROJECTS AND RESULTS •

https://cteq-tea.gitlab.io/

- CTEQ-TEA publications from INSPIRE
- LHAPDF grids for parton distributions
  - CT18 (N)NLO, CT18 QED, CT18 FC, …
  - Subtracted heavy-quark PDFs in the S-ACOT-MPS scheme
- Public codes
  - ePump (Hessian updating for PDFs with tolerance > 1)
  - LHAexplorer (fast surveys of data using L2 sensitivities)
  - Fantômas (Bezier parametrizations)
  - mp4lhc/mcgen (MC PDFs, combination of PDFs)
  - …

CT18up enhanced precision LHAPDF grids (2023)

On https://cteq-tea.gitlab.io/project/00pdfs/

- CT18, A, X, Z NNLO PDFs (2019 edition) presented as LHAPDF grids with a 1.9x higher number of x and Q nodes
- Same PDFs as in the LHAPDF library, with even more precise interpolation at $10^{-4} \leq x \leq 1$
- Recommended for high-mass and precision calculations; 2019 grids ok in other cases

Numbers of x, Q nodes in LHAPDF grids

intervals in Q	CT18	CT18up
$[Q_0, m_c]$	2	4
$[m_c, m_b]$	8	11
$[m_b, m_t]$	14	18
$[m_t, Q_{\max}]$	13	16
Total	37	49

intervals in x	CT18	CT18up	intervals in x	CT18	CT18up
$[10^{-10}, 10^{-9}]$	1	1	$[0.1, 0.2]$	7	18
$[10^{-9}, 10^{-8}]$	11	11	$[0.2, 0.3]$	6	16
$[10^{-8}, 10^{-7}]$	12	12	$[0.3, 0.4]$	5	12
$[10^{-7}, 10^{-6}]$	11	11	$[0.4, 0.5]$	3	13
$[10^{-6}, 10^{-5}]$	12	12	$[0.5, 0.6]$	6	15
$[10^{-5}, 10^{-4}]$	11	15	$[0.6, 0.7]$	6	12
$[10^{-4}, 10^{-3}]$	12	23	$[0.7, 0.8]$	8	11
$[10^{-3}, 10^{-2}]$	11	23	$[0.8, 0.9]$	14	17
$[10^{-2}, 0.1]$	12	40	$[0.9, 1]$	15	38
			Total	161	300

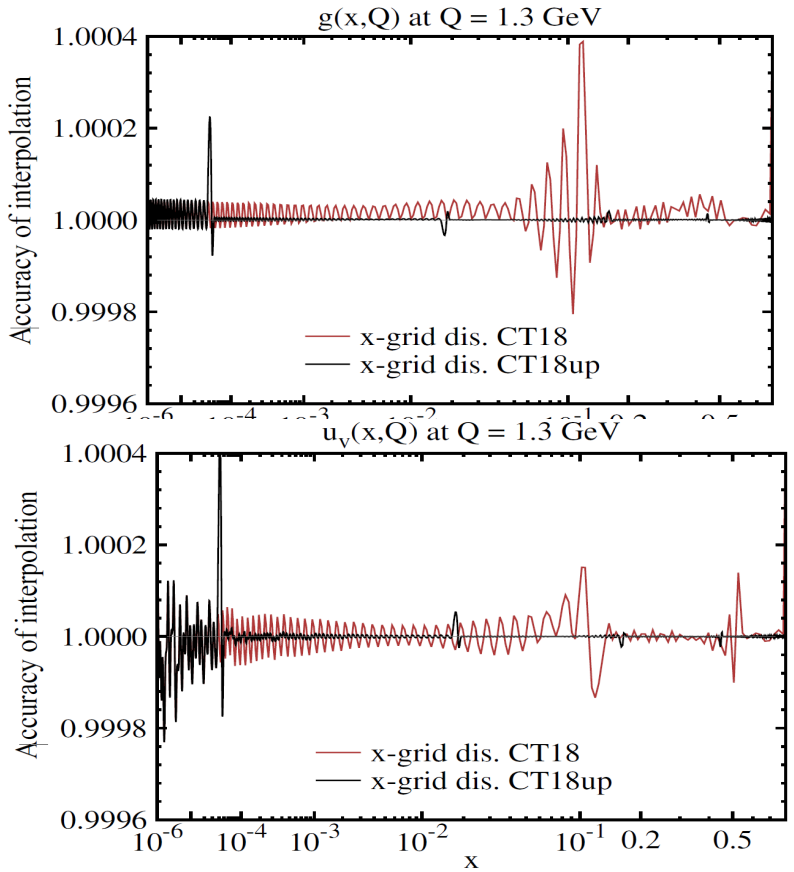

Toward a new generation of CT202X PDFs

1. Multiple preliminary NNLO fits with LHC Run-2 (di)jet, vector boson, $t\bar{t}$ data
   - based on the selections of experiments recommended in 2305.10733, 2307.11153
2. Next-generation PDF uncertainty quantification: Bézier curves, META combination, ML stress-testing, multi-Gaussian approaches, …
3. Physics applications
   a. QCD+QED PDFs for a neutron (K. Xie et al., 2305.10497)
   b. PDF dependence of forward-backward asymmetry (Y. Fu et al., 2307.07839)
   c. An L2 sensitivity study using xFitter (L. Kotz, 2401.11350)
   d. Fantômas Pion PDFs (L. Kotz et al., arXiv:2311.08447)
   e. AI/ML models for PDF generation (Kriesten and Hobbs, arXiv:2312.02278, 2407.03411)
4. Work on implementation of N3LO contributions

NNLO fits with new data at 8 and 13 TeV

Example

χ^2/N_{pt} for CT18+new data (CT18 in parentheses) NNLO fits; 68% CL

ID	Exp	N_{pt}	χ^2/N_{pt}
	Drell-Yan		
215	ATLAS 5.02 TeV W,Z	27	$0.82^{+0.55}_{-0.16}$ ($1.15^{+1.22}_{-0.43}$)
211	ATLAS 8 TeV W	22	$2.42^{+2.49}_{-1.51}$ ($4.25^{+6.39}_{-3.34}$)
214	ATLAS 8 TeV Z3D	188	$1.12^{+0.46}_{-0.02}$ ($1.99^{+5.10}_{-1.85}$)
212	CMS 13 TeV Z	12	$2.48^{+4.76}_{-0.88}$ ($12.03^{+38.04}_{-21.84}$)
217	LHCb 8 TeV W	14	$1.35^{+0.59}_{-0.61}$ ($1.35^{+0.72}_{-0.64}$)
218	LHCb 13 TeV Z	16	$1.18^{+1.42}_{-0.60}$ ($1.49^{+1.74}_{-0.89}$)
	13 TeV $t\bar{t}$		
521	ATLAS all-hadronic $y_{t\bar{t}}$	12	$1.06^{+0.14}_{-0.09}$ ($1.05^{+0.21}_{-0.10}$)
528	CMS dilep $y_{t\bar{t}}$	10	$1.10^{+1.08}_{-0.68}$ ($1.03^{+1.60}_{-0.74}$)
587	ATLAS lep+Jet $m_{t\bar{t}} + y_{t\bar{t}} + y^B_{t\bar{t}} + H_T^{t\bar{t}}$	34	$0.92^{+0.32}_{-0.14}$ ($0.94^{+0.59}_{-0.16}$)
581	CMS lep+jet $m_{t\bar{t}}$	15	$1.44^{+1.18}_{-0.73}$ ($1.37^{+1.86}_{-0.82}$)
	Inclusive Jet		
553	ATLAS 8 IncJet	171	$1.76^{+0.20}_{-0.12}$ ($1.80^{+0.33}_{-0.16}$)
554	ATLAS 13 IncJet	177	$1.38^{+0.13}_{-0.10}$ ($1.39^{+0.20}_{-0.11}$)
555	CMS 13 IncJet	78	$1.10^{+0.24}_{-0.17}$ ($1.11^{+0.30}_{-0.16}$)

nDY

nTT

nIncJet

nDYTTIncJet

Fits with 1 type of new data

A fit with all 3 types

PRELIMINARY

A 3-data-type fit (CT18+nDYTTIncJet)

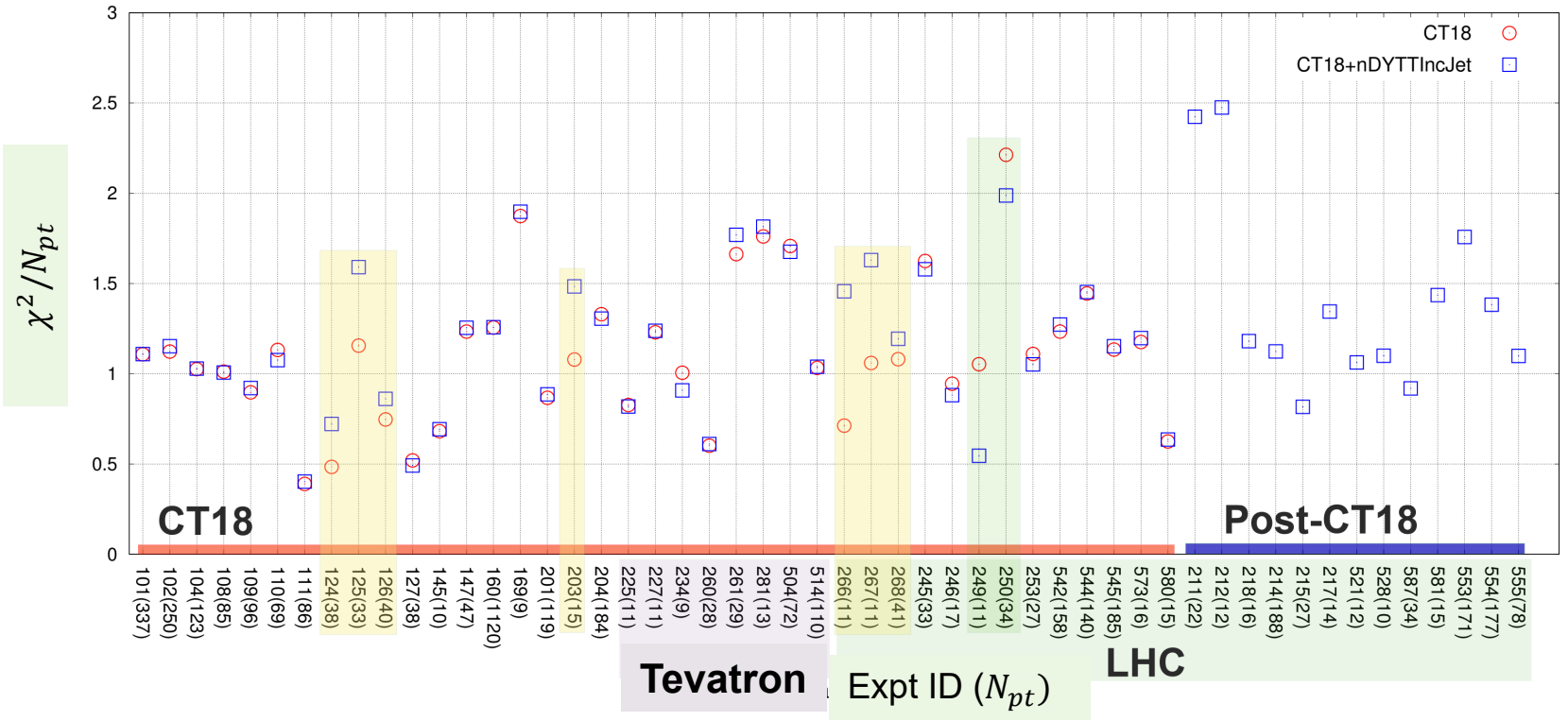

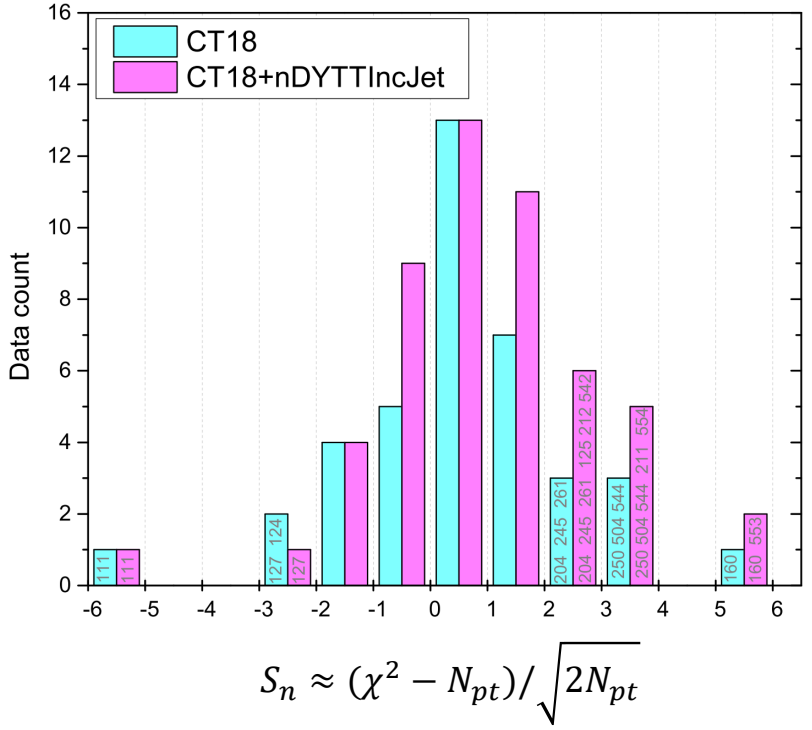

The most precise new experiments tend to have an elevated χ^2/N_{pt}, in the same pattern as observed for CT18

χ^2/N_{pt} increases for experiments 124 and 125 (NuTeV), 126 and 127 (CCFR) and 203 (E866 DY), 266 and 267 (CMS 7TeV Ach), 268 (ATLAS 7TeV W, Ach).

χ^2/N_{pt} decreases for experiments 249 (CMS 8 TeV Ach), 250 (LHCb 8 TeV W/Z)

Post-CT18 Drell-Yan data's impact

2305.10733 (PRD23')

ID	Experiment	N_{pt}	CT18	CT18A	CT18As
215	ATLAS 5.02 TeV W, Z	27	0.81	0.71	0.71
211	ATLAS 8 TeV W	22	2.45	2.63	2.51
214	ATLAS 8 TeV Z 3D†	188	1.12	1.14	1.18
212	CMS 13 TeV Z	12	2.38	2.03	2.71
216	LHCb 8 TeV W	14	1.34	1.36	1.43
213	LHCb 13 TeV Z	16	1.10	0.98	0.83
248	ATLAS 7 TeV W, Z	34	2.52	2.50	2.30
Total 3994/3953/3959 points			1.20	1.20	1.19

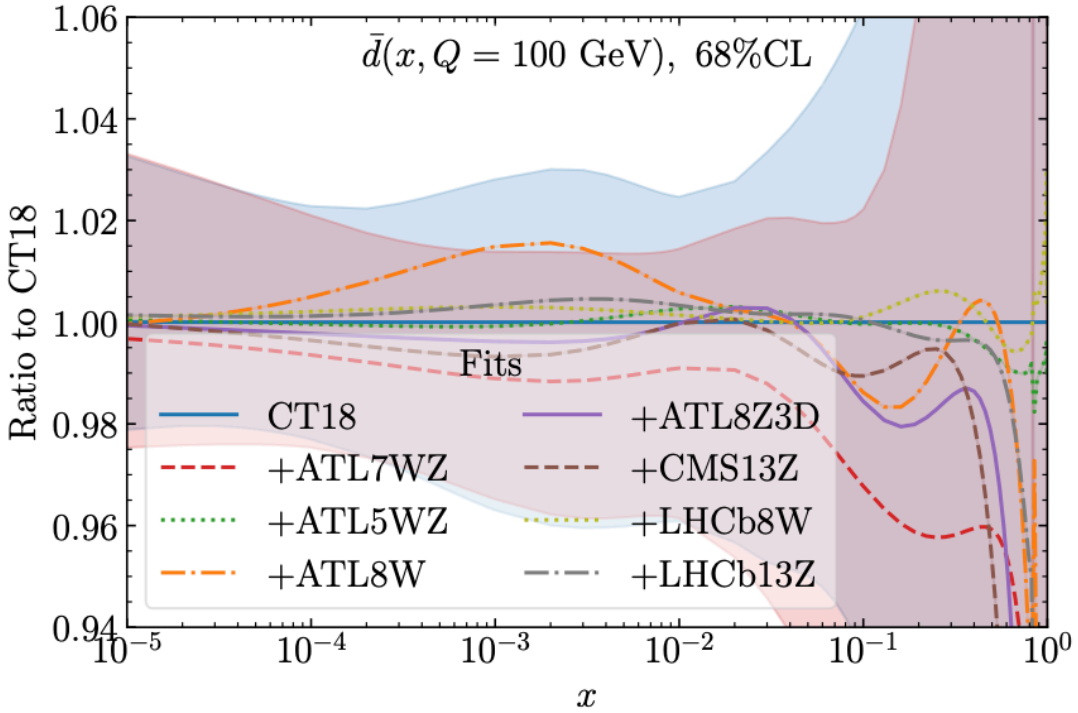

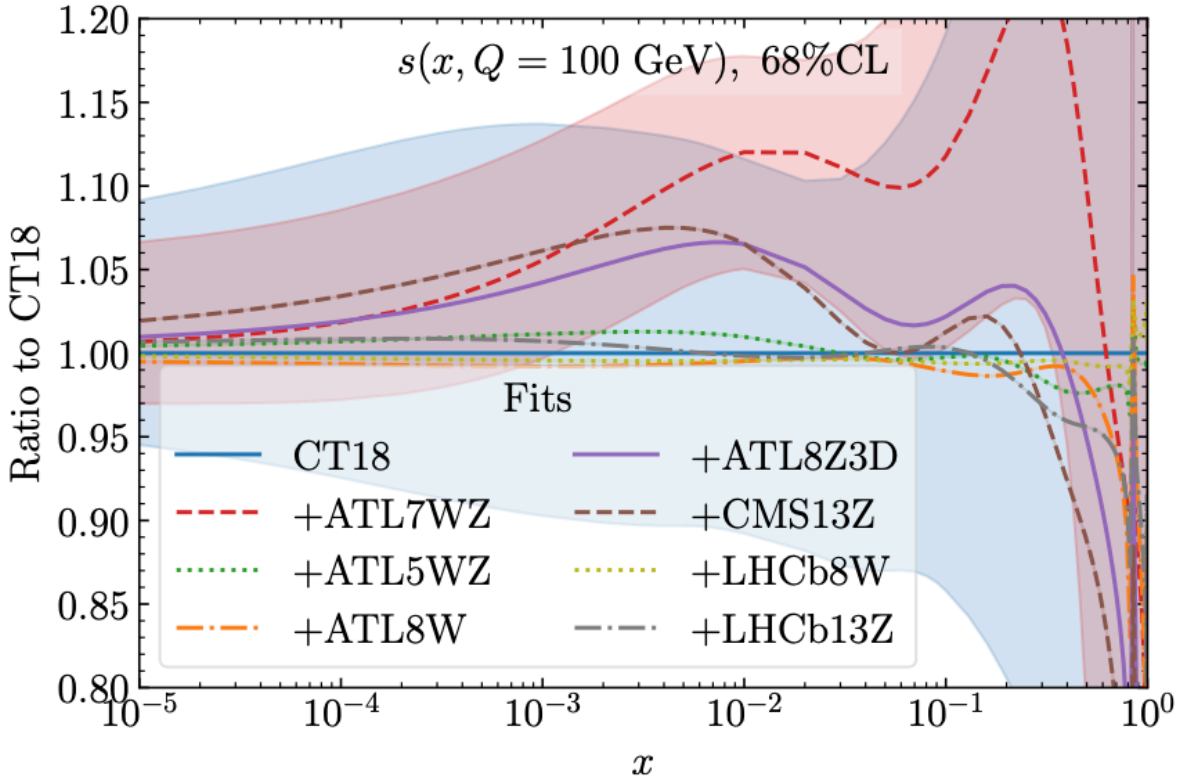

- Many new Drell-Yan (nDY) data came out after the release of CT18 PDFs.
- We found that most of the nDY data sets are consistent with the ATLAS 7 WZ precision data (16') and prefer enhanced strangeness at $x \sim 0.02$
- Only one exception: ATL8W has an opposite pull on $d, \bar{d}$
- CMS13Z and ATL8W have a similar χ^2/N_{pt} as ATL7WZ
- The more flexible strangeness parameterization in CT18As can relax the tension, but not completely resolve it.

Pulls on the gluon PDF by the new data type

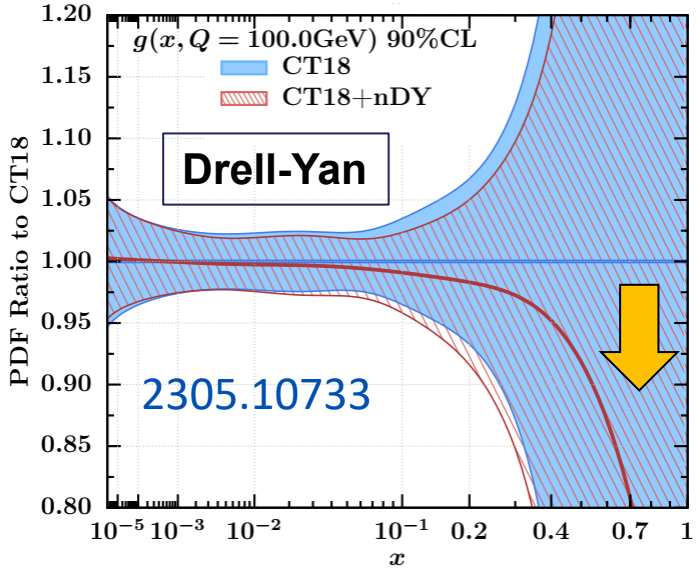

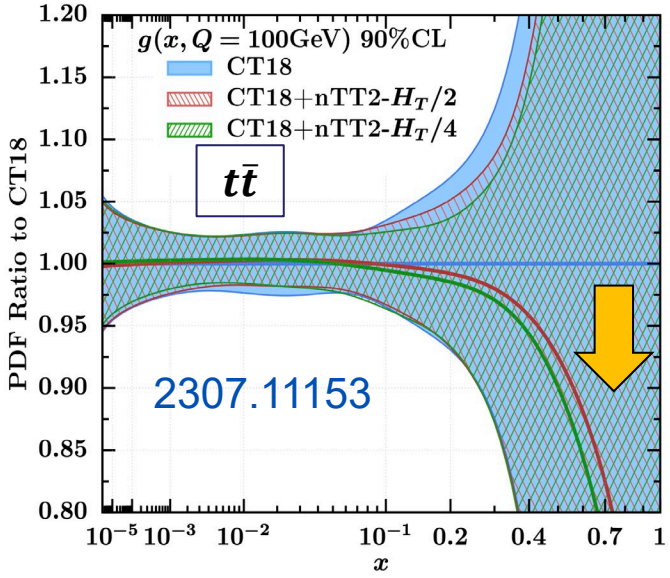

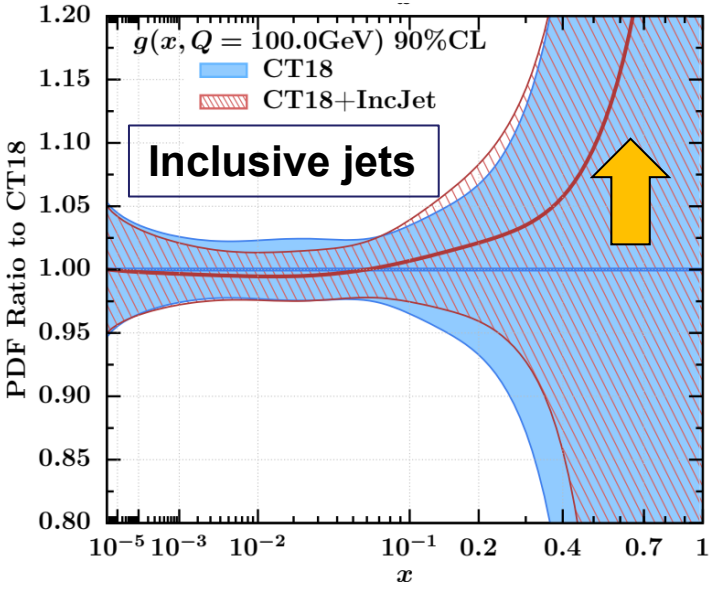

After including DY, $t\bar{t}$, and inc. jet data simultaneously, we get a softer gluon. Note that new DY and $t\bar{t}$ data favor a softer gluon, new inc. jet data prefer a harder gluon.

Mild changes in the gluon uncertainty

PRELIMINARY

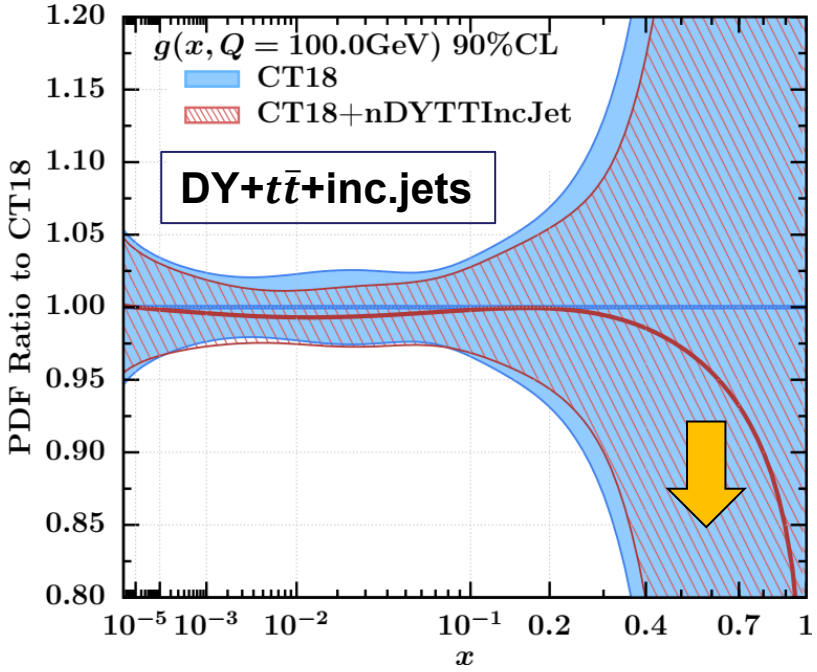

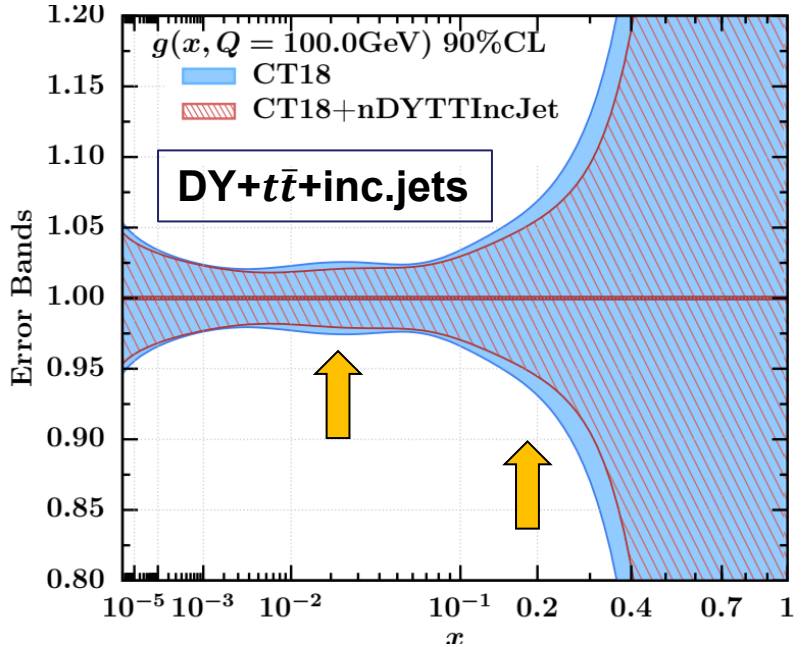

Correlations with PDFs in PVDIS at JLab 22 GeV

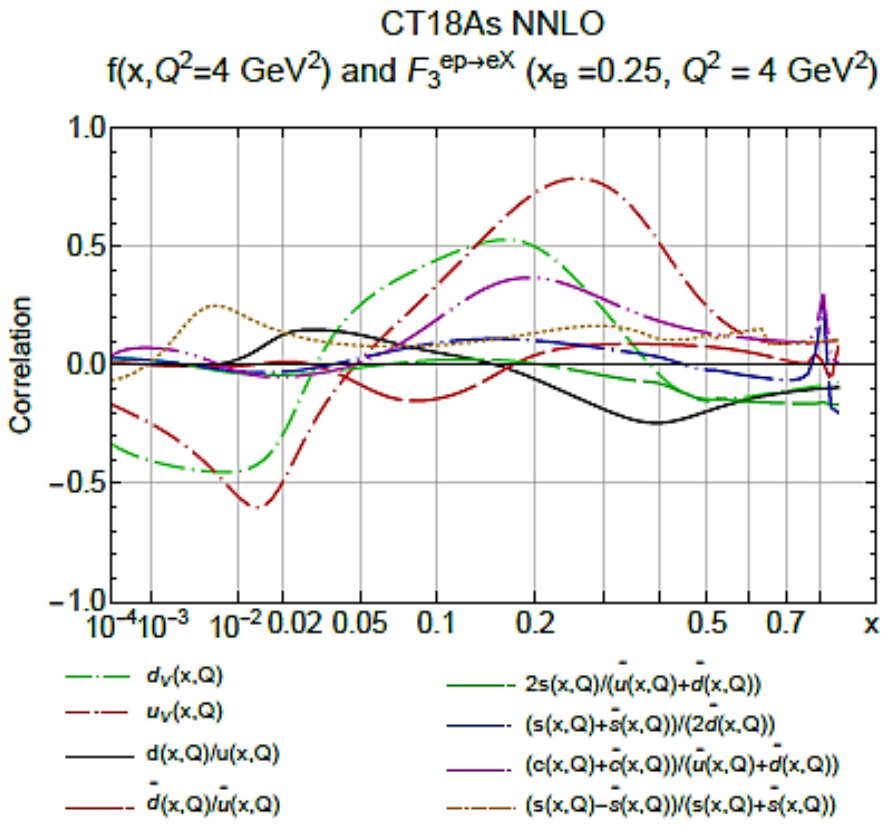

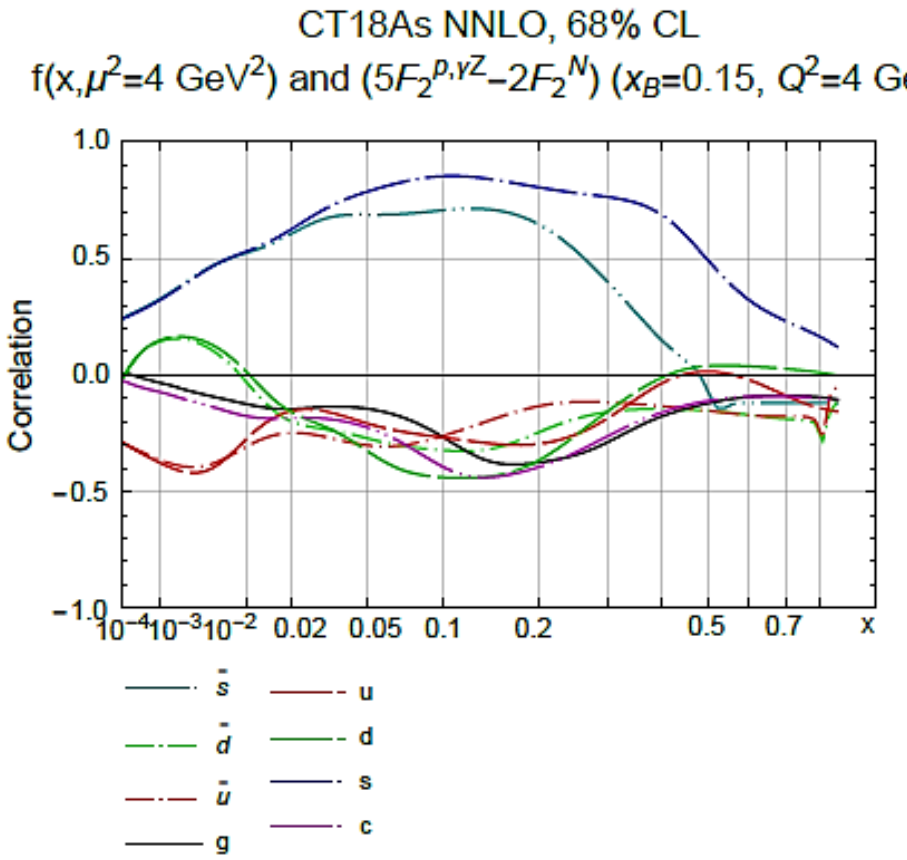

arXiv:2306.09360
arXiv:2408.04020

Observe a large correlation of PVDIS with strangeness; how large is the actual data sensitivity?

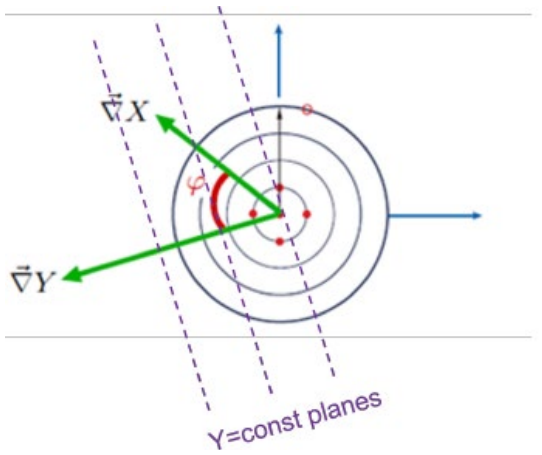

Figure 16: When combined with other high-energy observables in a QCD global fit, parity-violating lepton scattering may access unique quark charge-flavor currents to help disentangle the flavor dependence of the nuclear sea at high x. In the upper row, we plot the Hessian correlations of (a) several PDF flavor combinations with the parity-violating structure function $F_3(x_B, Q)$ and (b) the individual PDF flavors and a combination $5F_2^{\gamma Z,p}(x_B, Q) - 2F_2^N(x_B, Q)$ with a potential sensitivity to strangeness. (c) We illustrate

Sensitivities to PDFs in PVDIS at JLab 22 GeV

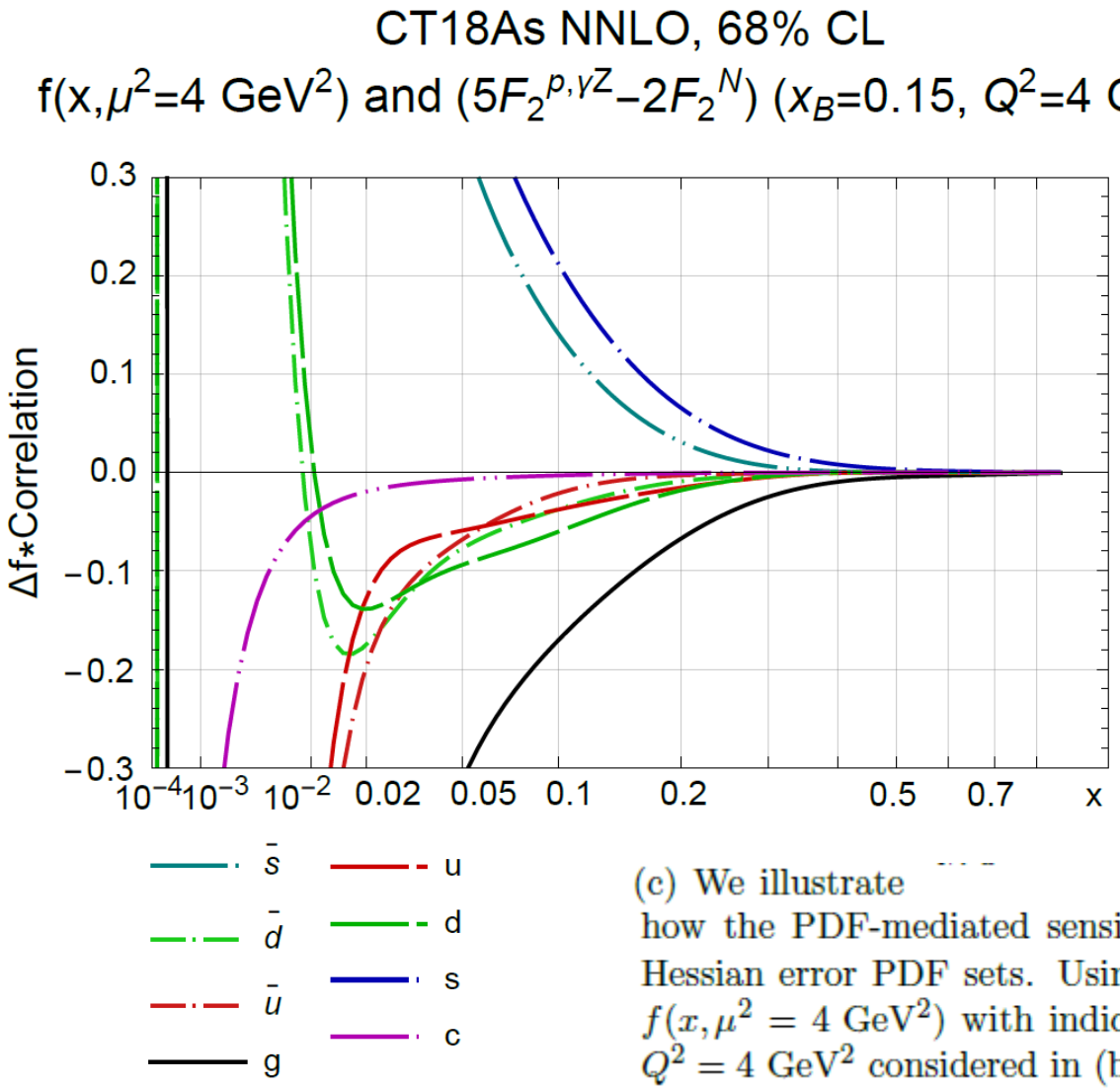

arXiv:2408.04020

A NEW TECHNIQUE;
shows that PVDIS determination of strangeness requires tight external constraints on gluon and dbar PDFs

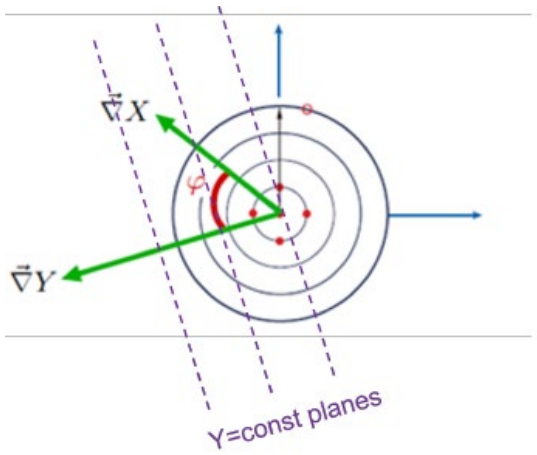

(c) We illustrate how the PDF-mediated sensitivity of Y to X can be estimated using the gradients computed with the Hessian error PDF sets. Using this technique, panel (d) estimates the sensitivity of constraints on PDFs $f(x, \mu^2 = 4\ \mathrm{GeV}^2)$ with indicated flavors to the combination $5F_2^{\gamma Z,p}(x_B, Q) - 2F_2^N(x_B, Q)$ at $x_B = 0.15$, $Q^2 = 4\ \mathrm{GeV}^2$ considered in (b).

Accurate (NNLO) PDFs

CT18 NNLO/CT18Z NNLO

MSHT20, NNPDF3.1/4.0 NNLO
ABMP, ATLAS, … NNLO

→ multiple PDF solutions consistent with observations

Potentially more accurate (aN3LO) PDFs

MSHT20 aN3LO

NNPDF4.0 aN3LO

→ Different from NNLO?
More consistent?
Unique?

→ **"NNLO+"**

Mixed NNLO-N3LO calculations

E.g., a possible CT18 NNLO+ prescription (out of several)

1. Use CT18Z NNLO or CT18 NNLO error sets
2. Central prediction: take the average of predictions with $\hat{\sigma}_{NNLO}$ and $\hat{\sigma}_{N3LO}$
3. Scale uncertainty: compute using $\hat{\sigma}_{N3LO}$

How different from aN3LO predictions?

Necessary components of an N3LO PDF analysis

Component		Availability
Splitting functions		Partial N3LO
Hard cross sections	• DIS, light flavors	Full N3LO
	• NC DIS, heavy flavors	Full N3LO (Blümlein et al.), not yet in fitting codes
	• Vector boson production	Full N3LO for some processes, fixed N3LO/NLO K-factor tables
	• CC DIS, jet, $t\bar{t}$ production	N2LO
	• $pp \to W + c$, $pp \to Z + b$, $\mathrm{pp} \to b$	NLO (massive); NNLO (ZM)

Looking forward to including all components **exactly and fully** to reduce the QCD scale uncertainty and guarantee the N3LO accuracy in the near future.

CTEQ-TEA and other groups include some N3LO contributions in their fitting codes: recent progress of MSHT and NNPDF in NNLO+ (aN3LO) fits

QCD cross sections @N3LO

Work in progress

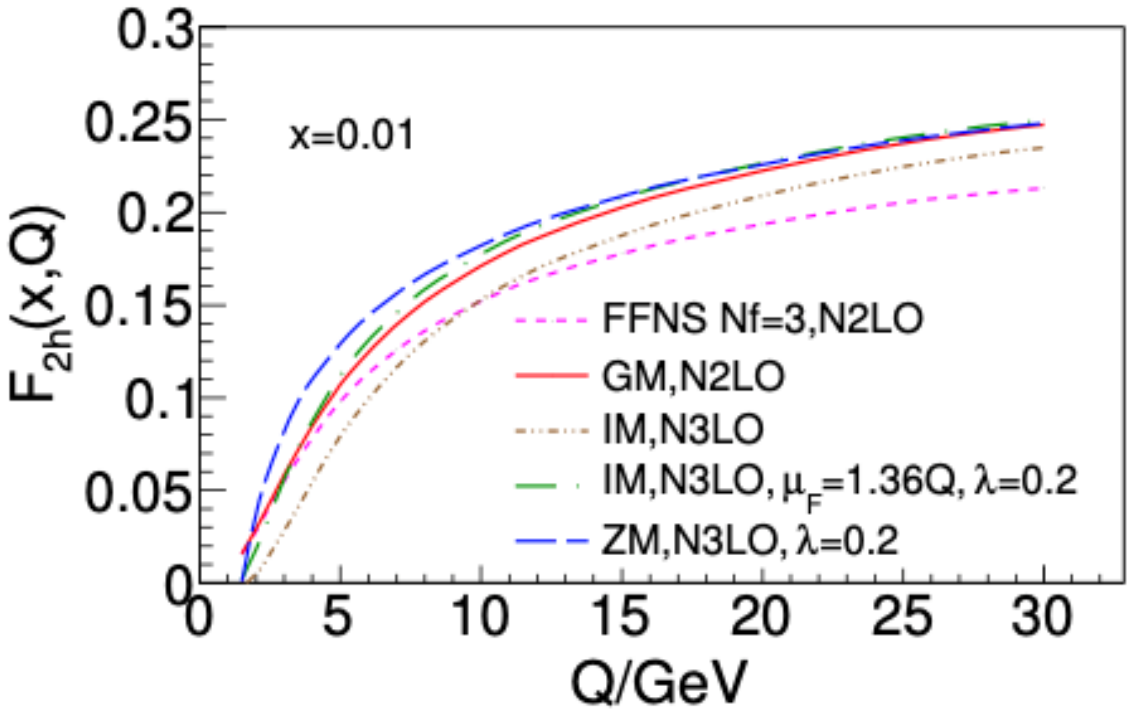

- **DIS:** The CTEQ-TEA code implements complete flavor decompositions of DIS SFs at N3LO using approximate zero-mass Wilson coefficients with a rescaling variable (the **Intermediate-Mass VFN scheme**, cf. the figure)

Boting Wang's and Keping Xie's Theses, SMU

- **Working on the implementation of** massive N3LO heavy-quark coefficients to obtain N3LO DIS cross sections in **the SACOT-MPS General-Mass VFN scheme**

Factorization schemes	Mass dependence in the FC terms	Mass dependence of the FE and subtraction terms	Introduce heavy-quark PDFs at large Q
FFN	Exact	N/A	no
ZM	None	None	yes
IM	Approximate	Approximate	yes
GM	Exact	Approximate	yes

- **DGLAP evolution** is performed at N3LO with APFEL/APFEL++.
- **Drell-Yan:** Ongoing work to include N3LO DY effects using NNLO ApplFast + N3LO/N2LO K-factor tables

Probing parton luminosities with toy N3LO cross sections

Computations done by Max Ponce Chavez

Compute NNLO, N3LO cross sections with the n3loxs code (Baglio et al., 2209.06138)

1. Test gg luminosities via $gg \to$ toy H^0X; heavy top-quark limit with $N_f = 5$
2. Test $q\bar{q}$ luminosities via $q\bar{q} \to$ toy $Z'X$

- Retain SM couplings; vary masses $M_{H,Z'}$ to test $f_a(x,\mu)$ at $x \sim \frac{M_{H,Z'}}{\sqrt{s}}$
- Estimate the 7-point QCD scale uncertainty around $\mu_{F,0} = \mu_{R,0} = M_H$ or $M_H/2$ for Higgs, $\mu_{F,0} = \mu_{R,0} = M_{Z'}$ for Z'.
- do not include the PDF uncertainty
  - Do the included N3LO contributions add up or cancel in the hadronic cross sections?

$pp \rightarrow$ toy H^0X, central scales $\mu_{F0} = \mu_{R0} = M_H$

See $\mu_{F0} = \mu_{R0} = M_H/2$ in the supplemental .pdf file
(default choice in n3loxs, asymmetric 7pt errors)

All figures are preliminary!

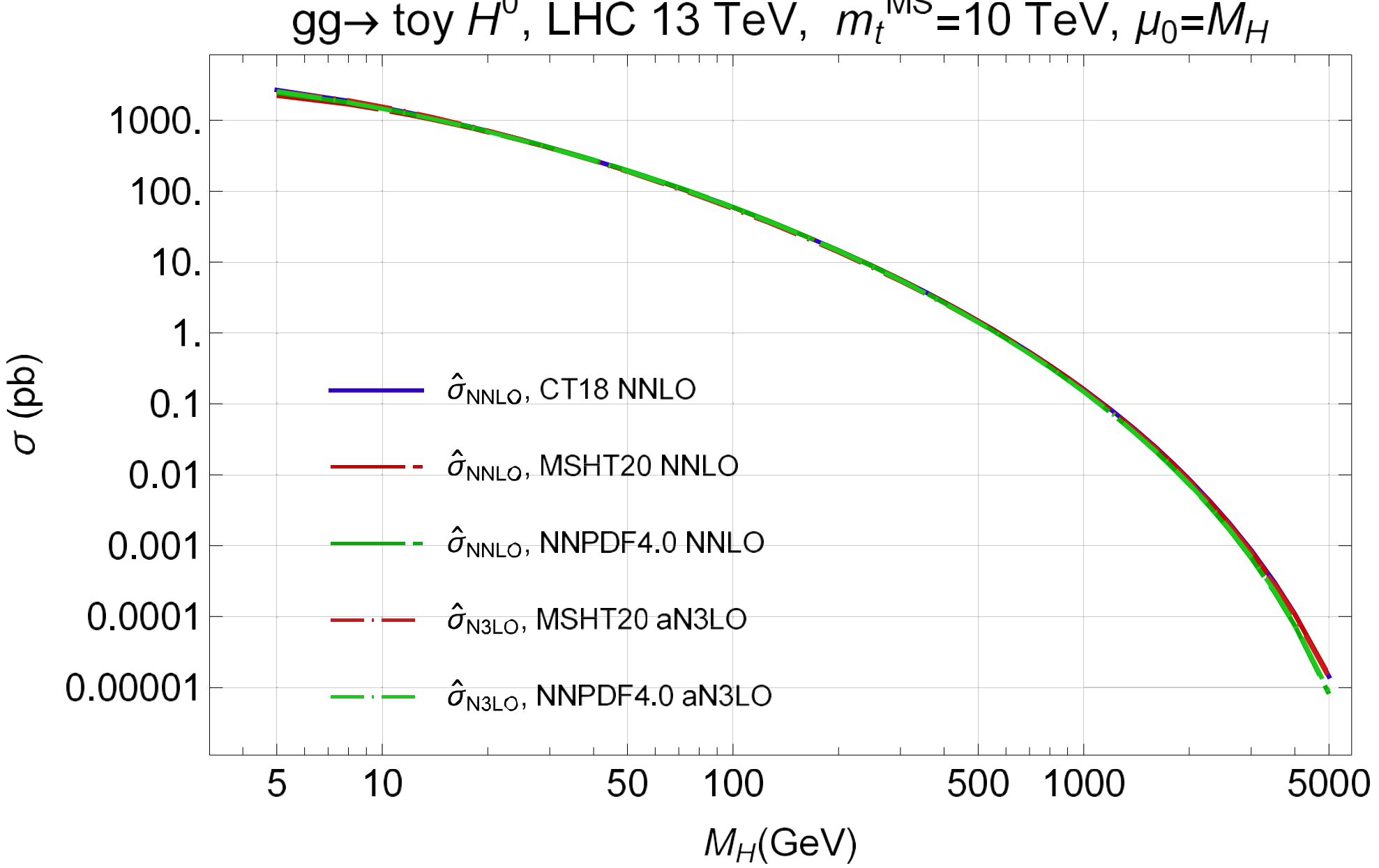
gg→ toy H^0, LHC 13 TeV, $m_t^{\overline{MS}}$=10 TeV, $\mu_0=M_H$
σ (pb)
1000.
100.
10.
1.
0.1
0.01
0.001
0.0001
0.00001
$\hat{\sigma}_{NNLO}$, CT18 NNLO
$\hat{\sigma}_{NNLO}$, MSHT20 NNLO
$\hat{\sigma}_{NNLO}$, NNPDF4.0 NNLO
$\hat{\sigma}_{N3LO}$, MSHT20 aN3LO
$\hat{\sigma}_{N3LO}$, NNPDF4.0 aN3LO
5
10
50
100
500
1000
5000
M_H(GeV)

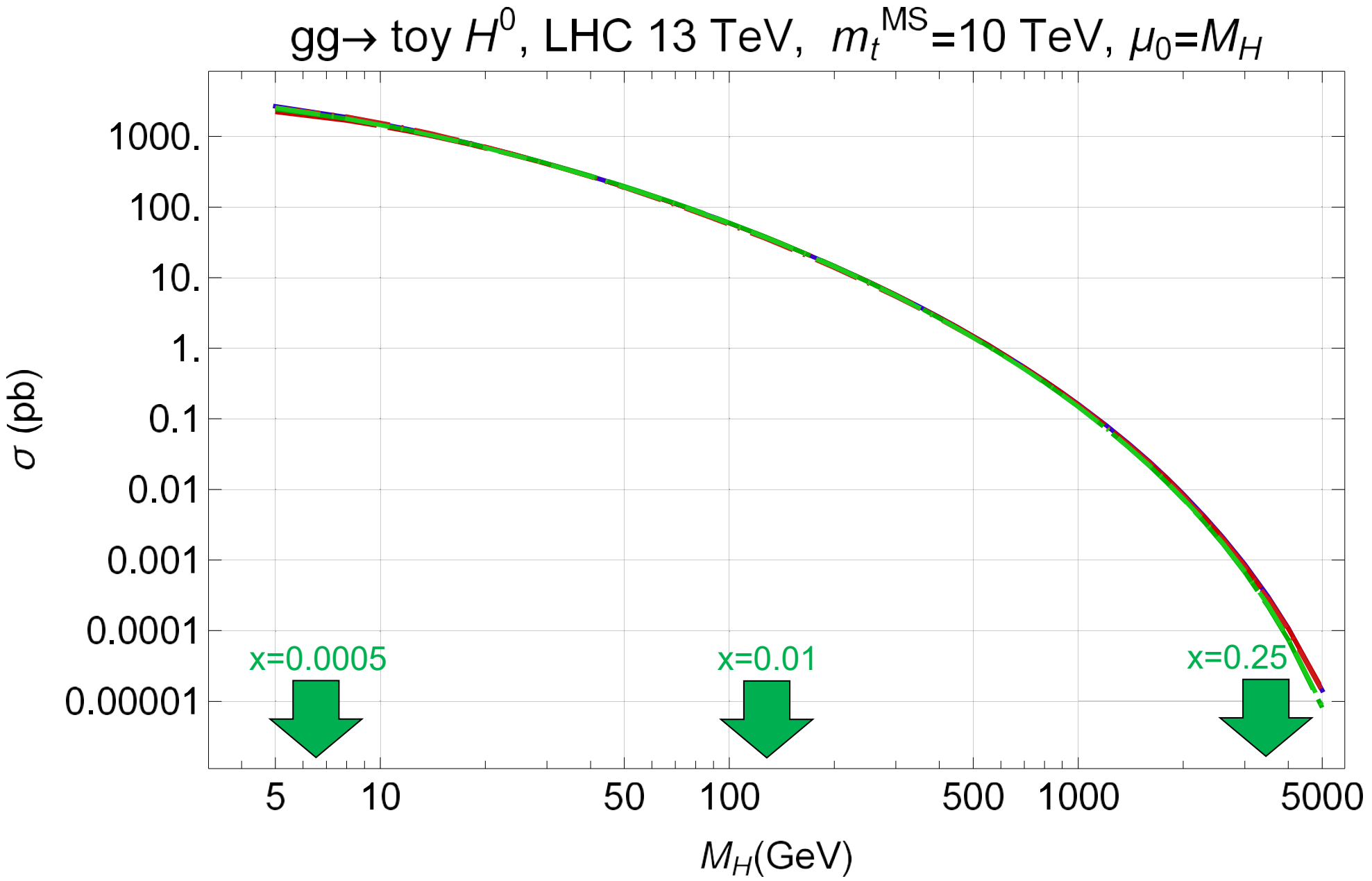
gg→ toy H^0, LHC 13 TeV, $m_t^{\overline{MS}}$=10 TeV, μ_0=M_H
σ (pb)
1000.
100.
10.
1.
0.1
0.01
0.001
0.0001
0.00001
x=0.0005
x=0.01
x=0.25
5
10
50
100
500
1000
5000
M_H(GeV)

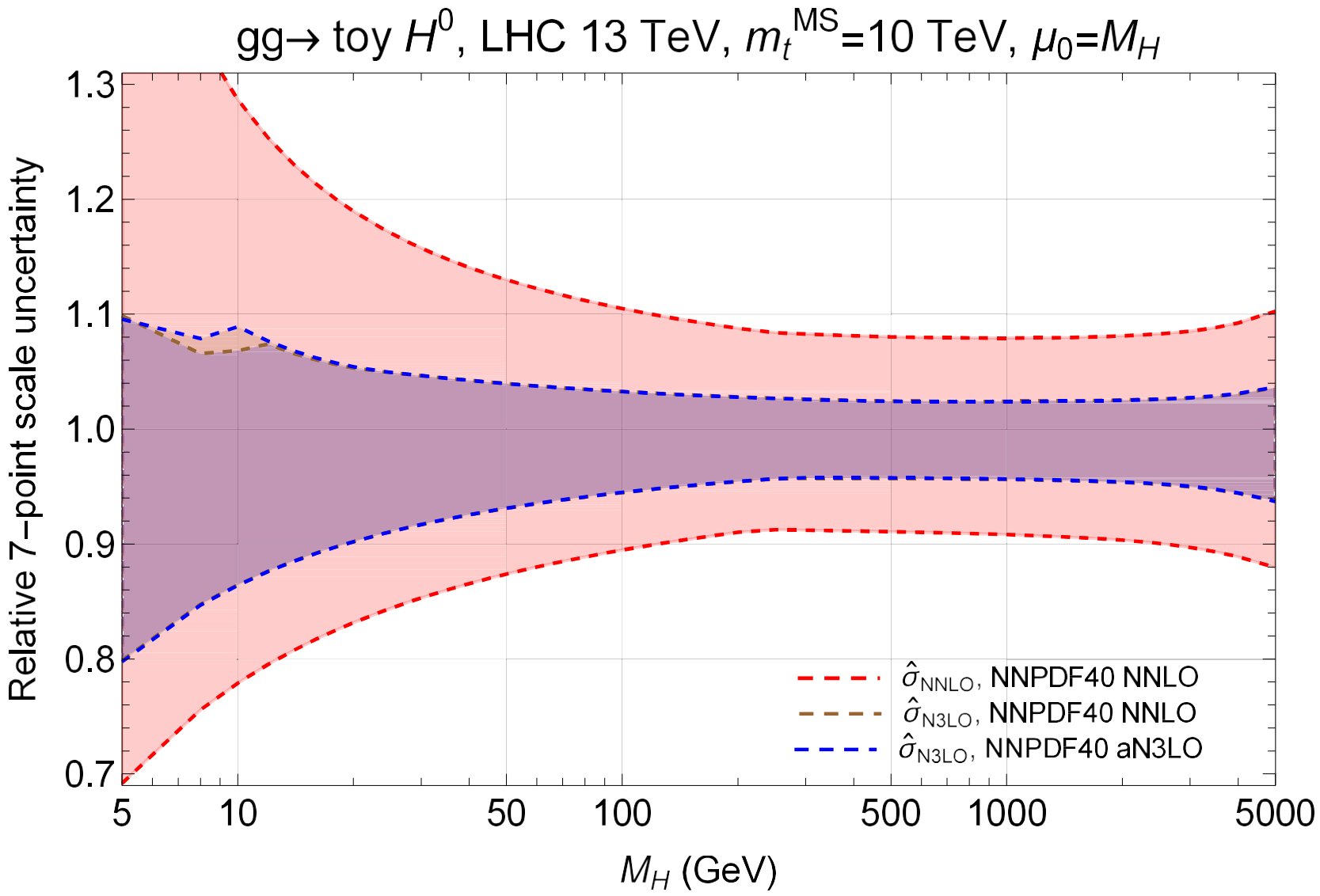

N3LO scale uncertainty is about the same with either NNLO or aN3LO PDFs

At $M_H \approx 10$ GeV, more variability due to the $b\bar{b}$ mass threshold

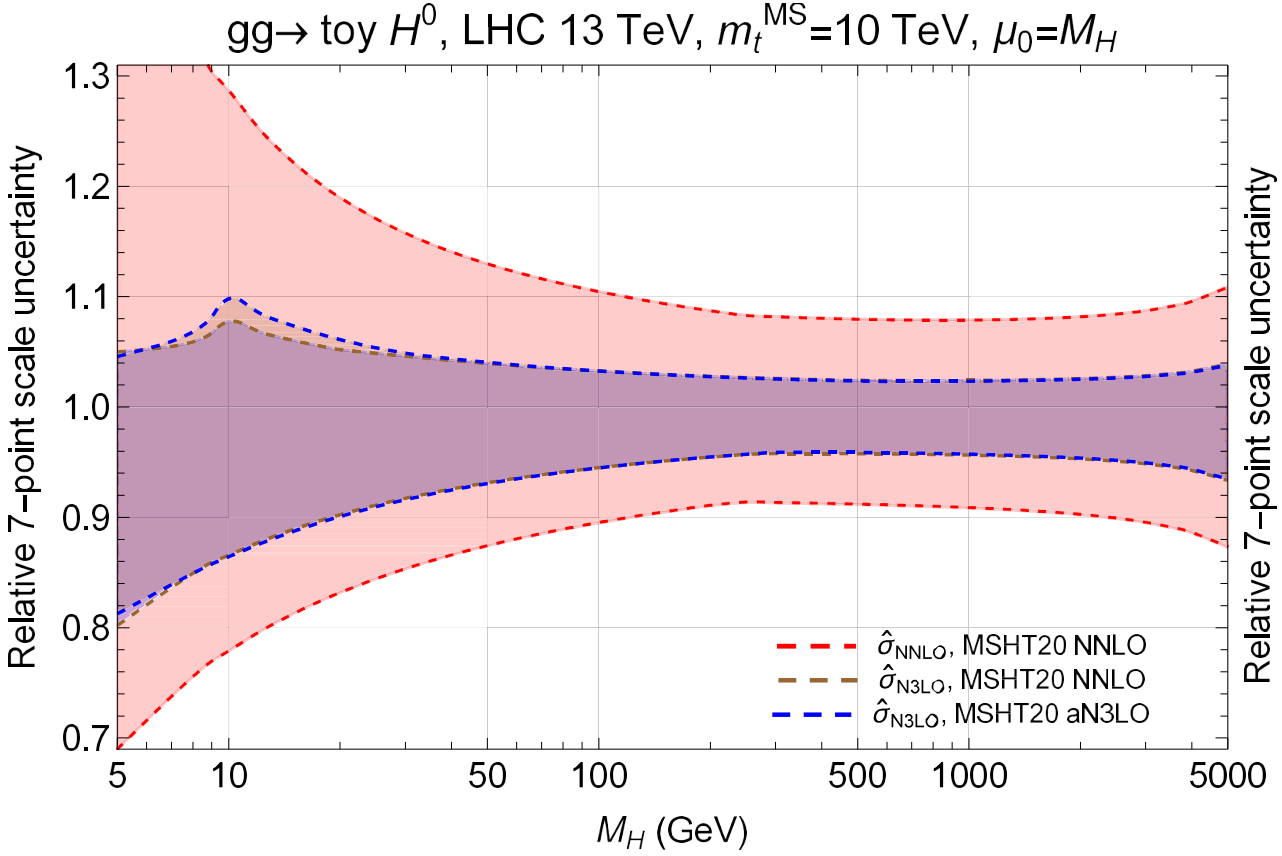

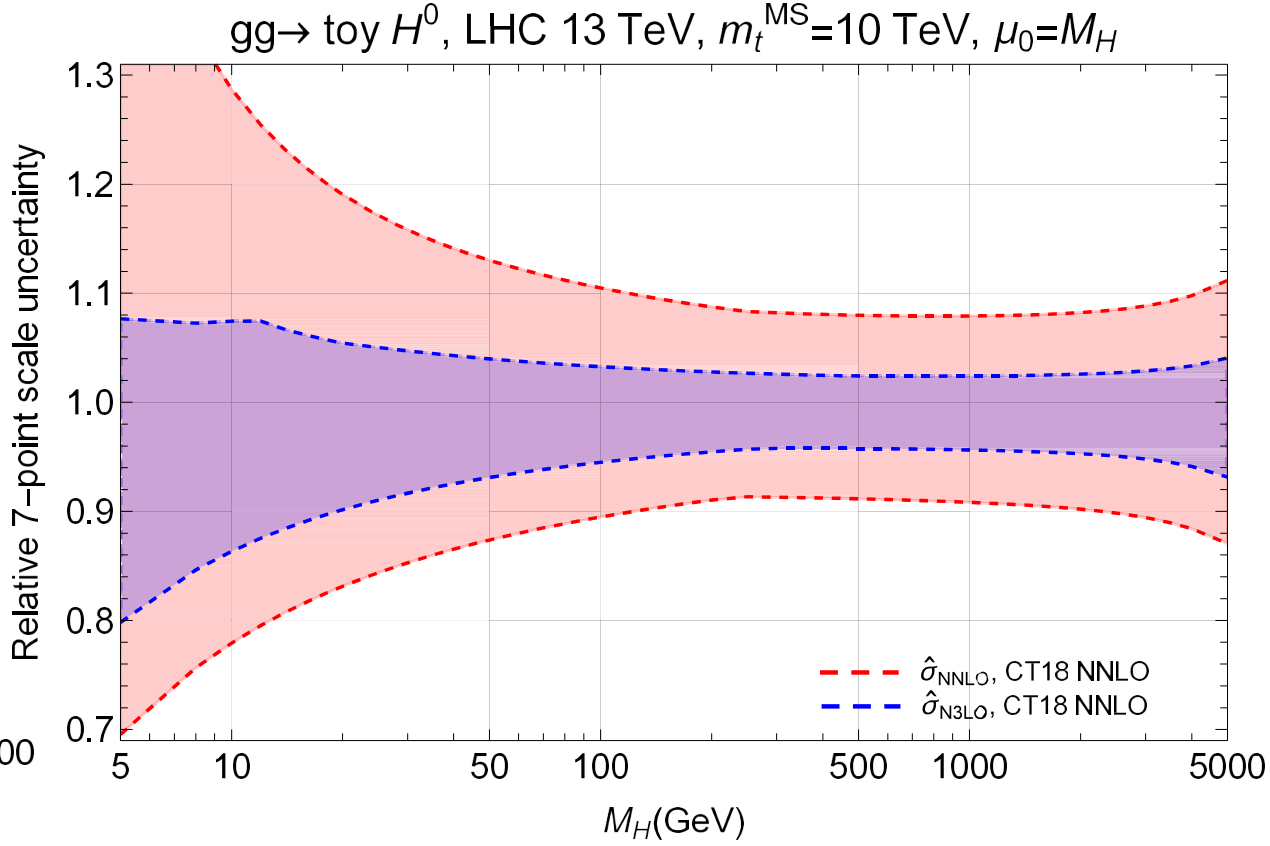

N3LO scale uncertainty is about the same with either NNLO or aN3LO PDFs

NNLO+ vs NNLO

Normalized to the average of NNLO and NNLO+ cross sections

CTEQ-TEA “NNLO+” correction is similar to the two aN3LO ones

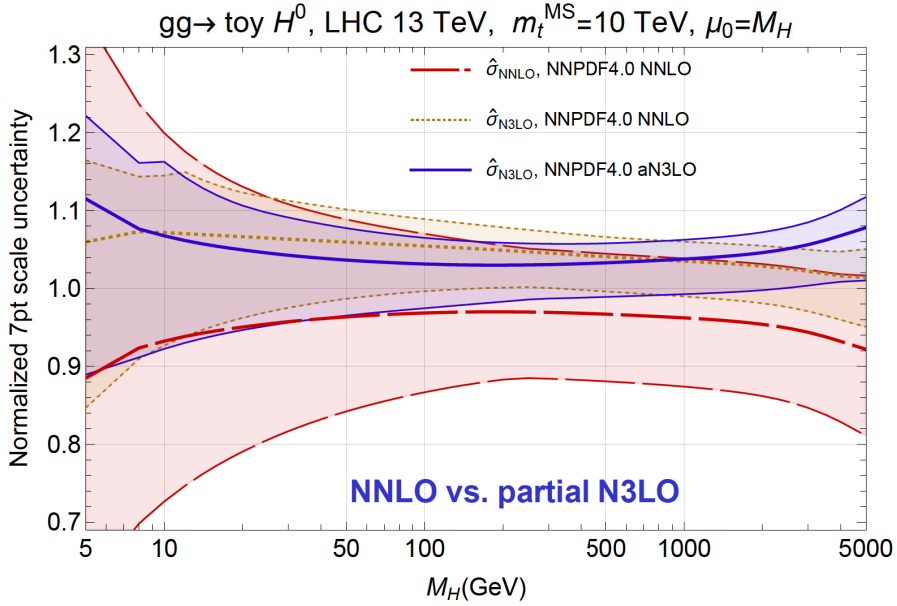

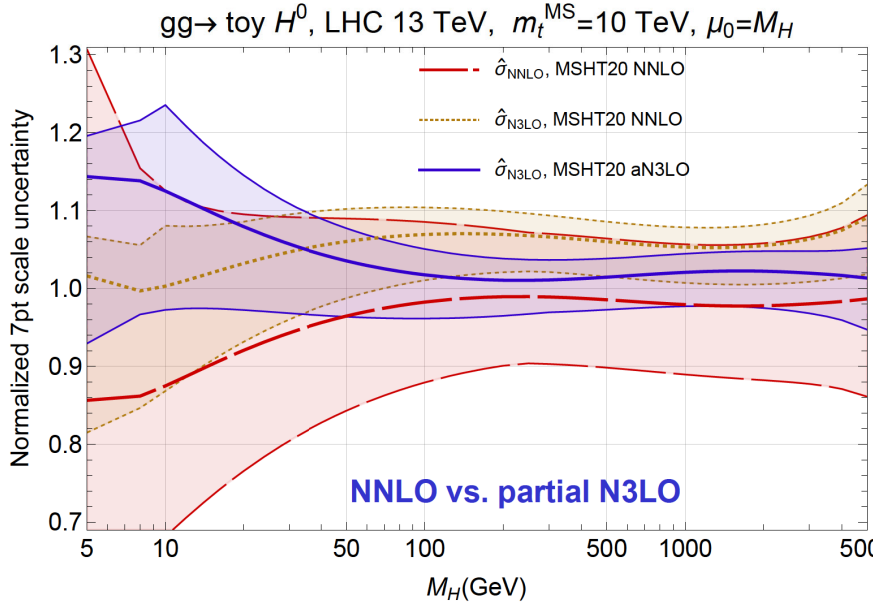

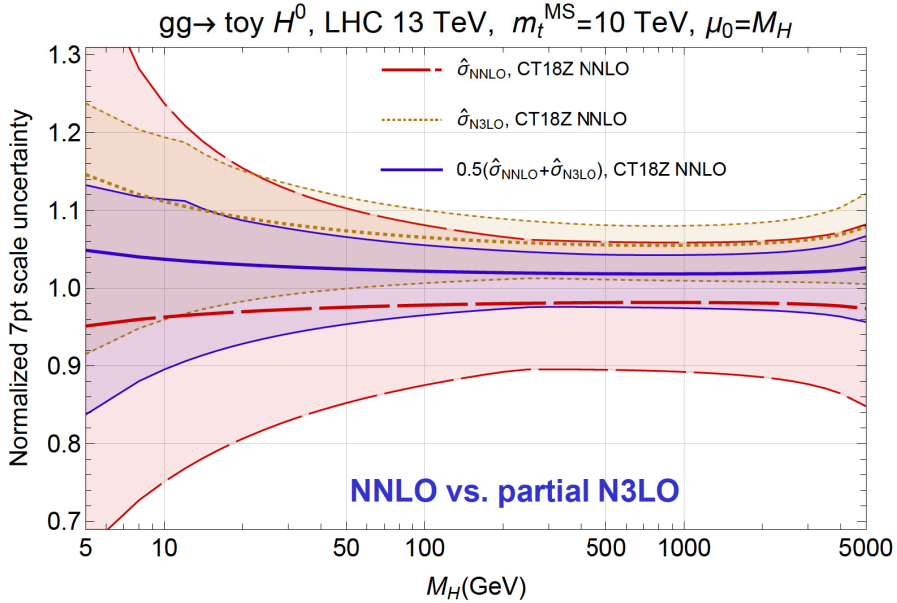

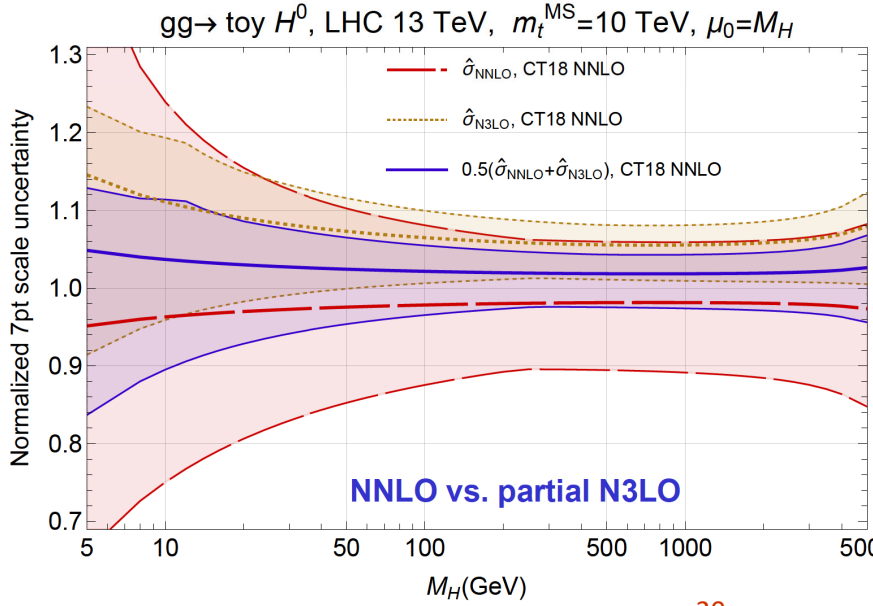

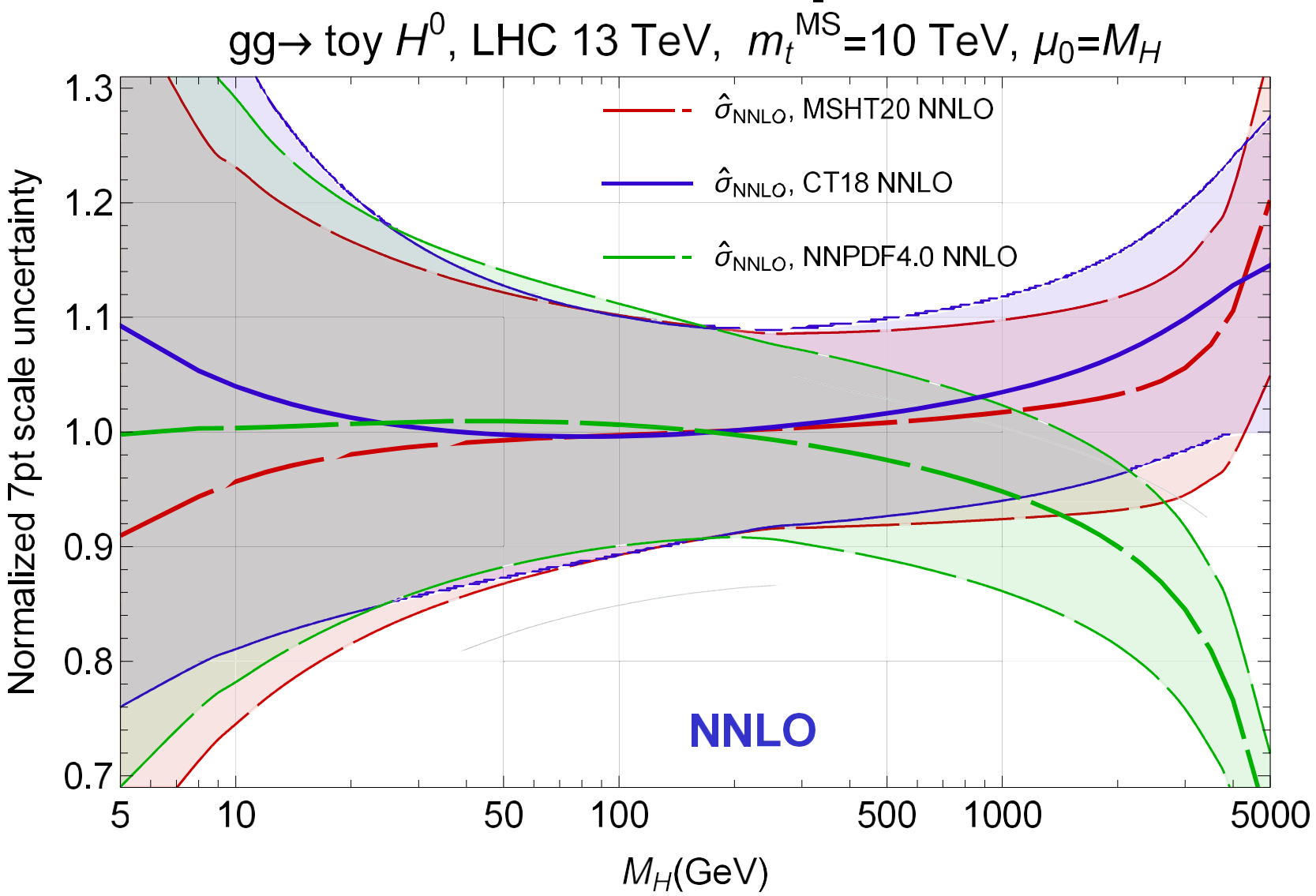

Scale uncertainty bands normalized by the average of central CT18, MSHT20, NNPDF4.0 cross sections

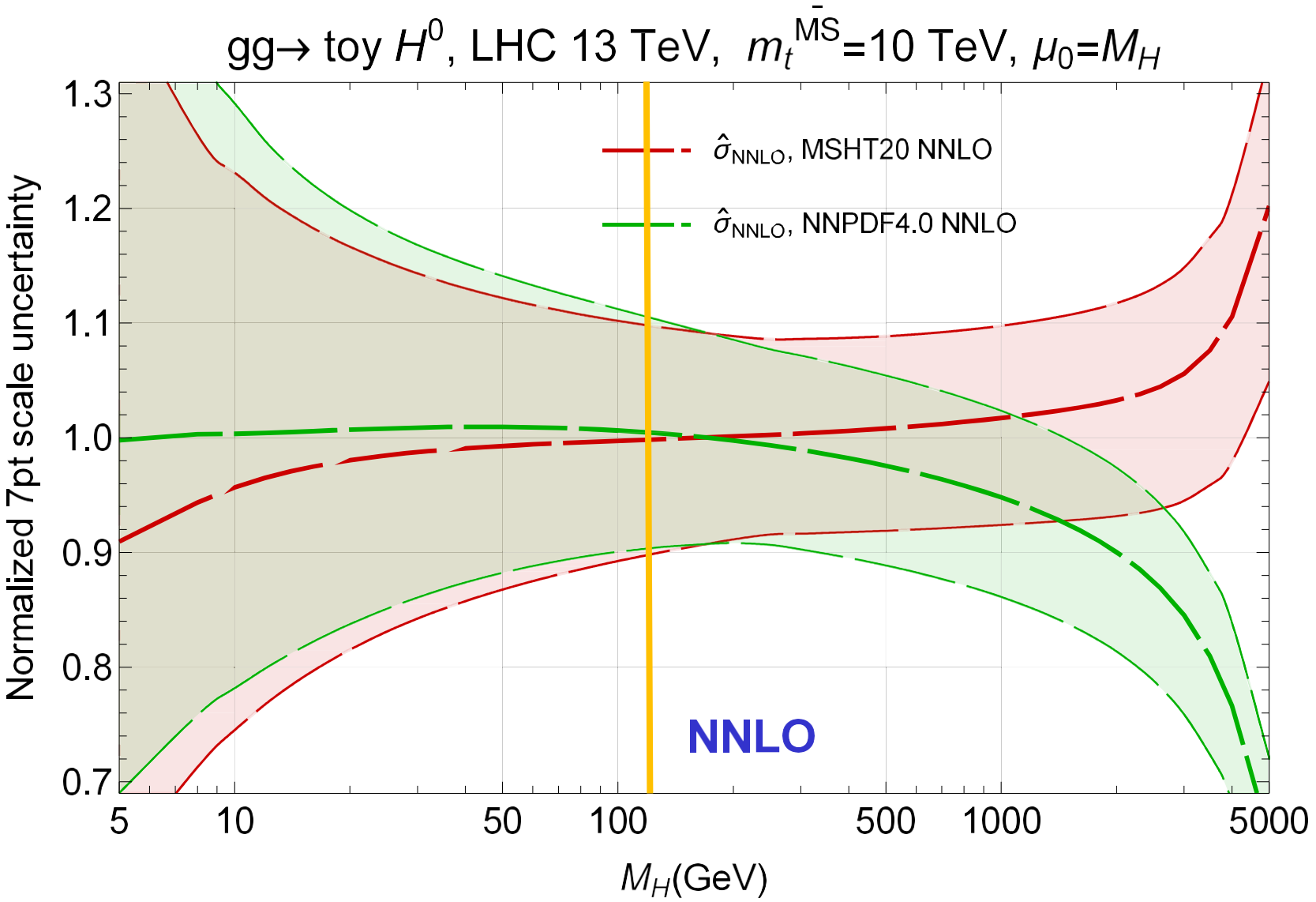
gg→ toy H^0, LHC 13 TeV, $m_t^{\bar{MS}}$=10 TeV, $\mu_0=M_H$
$\hat{\sigma}_{NNLO}$, MSHT20 NNLO
$\hat{\sigma}_{NNLO}$, NNPDF4.0 NNLO
NNLO
Normalized 7pt scale uncertainty
1.3
1.2
1.1
1.0
0.9
0.8
0.7
5
10
50
100
500
1000
5000
M_H(GeV)

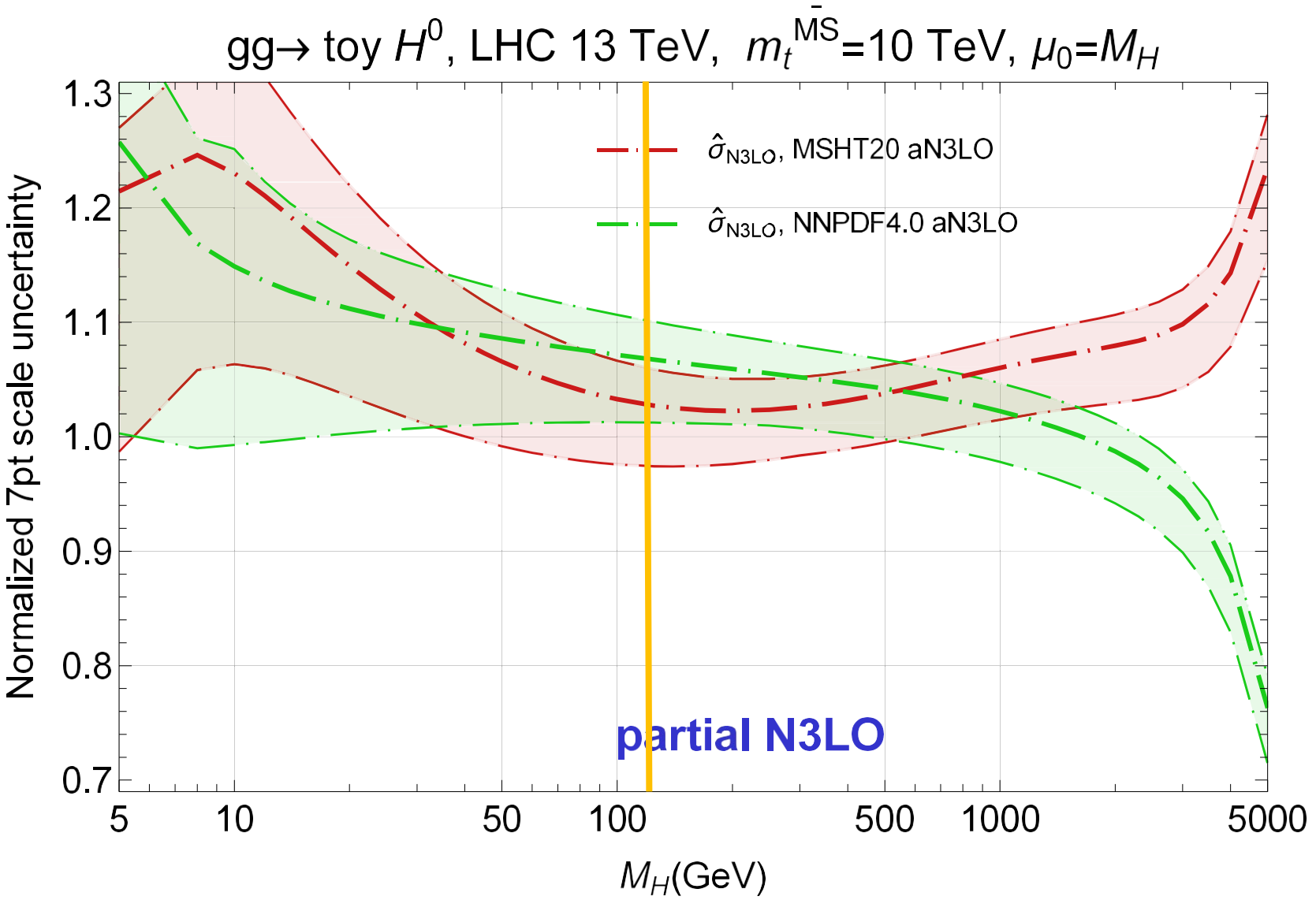

Enlarged $g(x)$ at $x < 10^{-3}$

Weaker agreement at $M_H = 125$ GeV than at NNLO

Persistent differences at $x > 0.1$ reflect tensions in fitted data

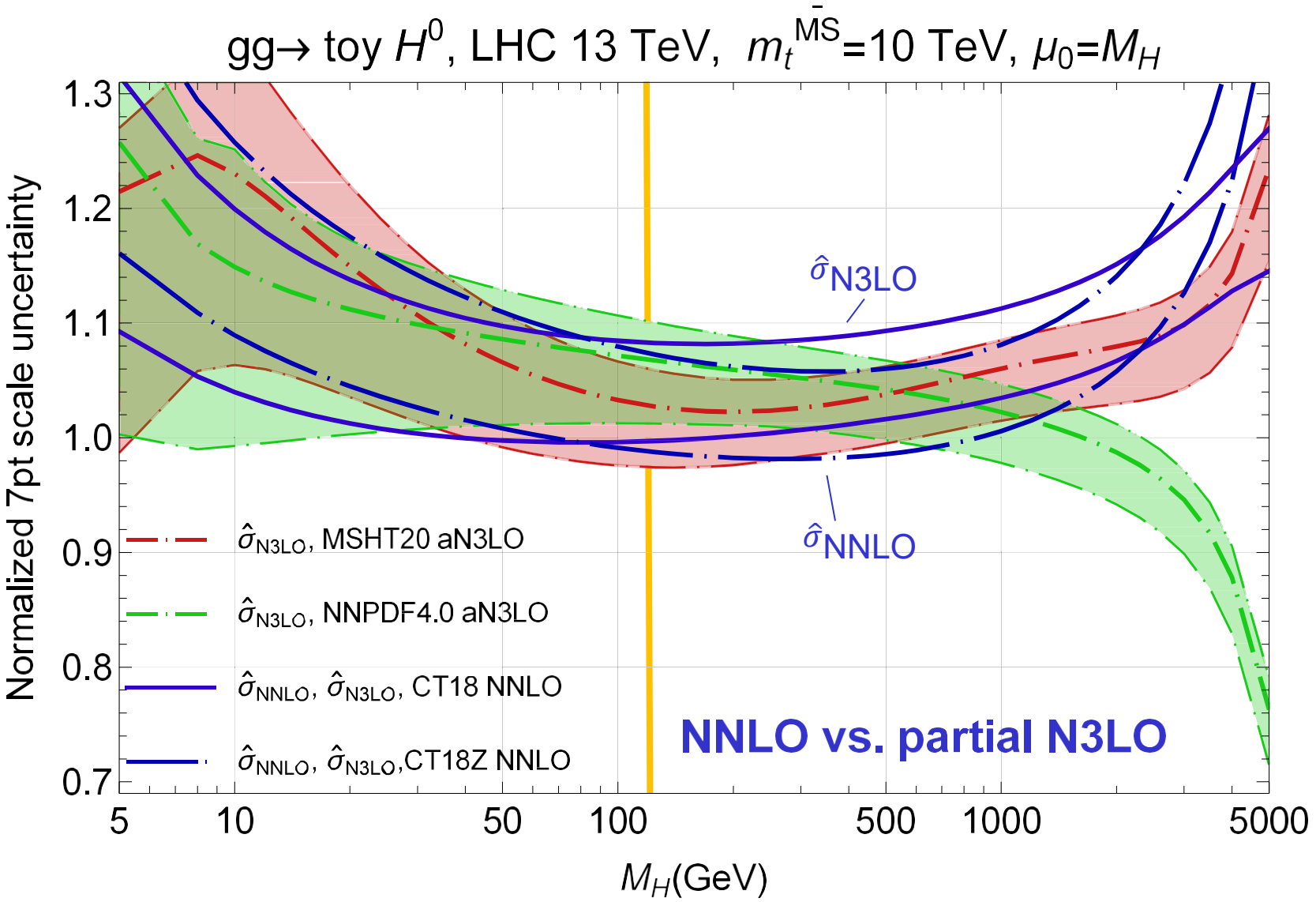
gg→ toy H^0, LHC 13 TeV, $m_t^{\overline{MS}}$=10 TeV, $\mu_0=M_H$
Normalized 7pt scale uncertainty
1.3
1.2
1.1
1.0
0.9
0.8
0.7
5
10
50
100
500
1000
5000
M_H(GeV)
$\hat{\sigma}_{N3LO}$
$\hat{\sigma}_{NNLO}$
$\hat{\sigma}_{N3LO}$, MSHT20 aN3LO
$\hat{\sigma}_{N3LO}$, NNPDF4.0 aN3LO
$\hat{\sigma}_{NNLO}$, $\hat{\sigma}_{N3LO}$, CT18 NNLO
$\hat{\sigma}_{NNLO}$, $\hat{\sigma}_{N3LO}$,CT18Z NNLO
NNLO vs. partial N3LO

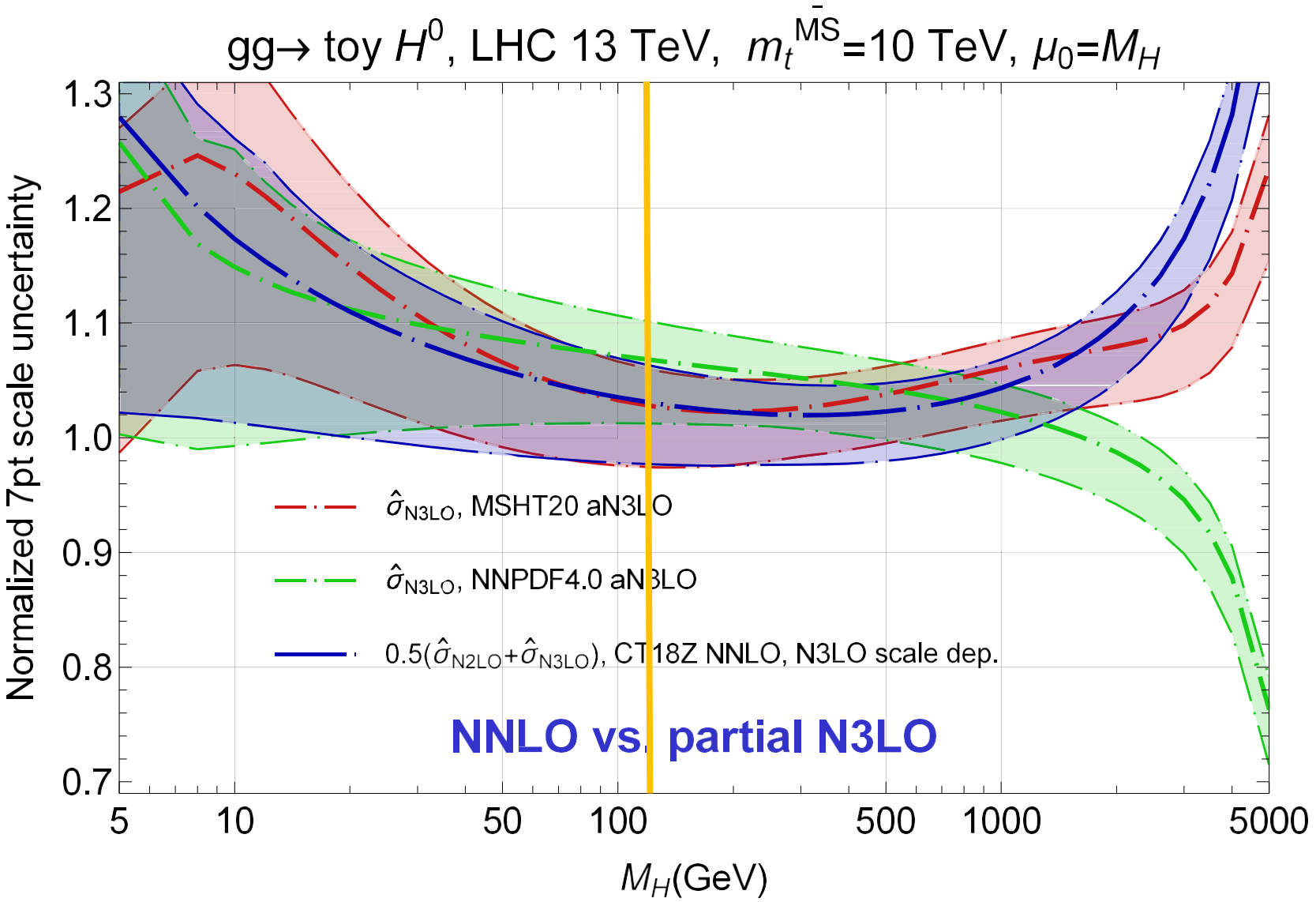
gg→ toy H^0, LHC 13 TeV, $m_t^{\overline{MS}}$=10 TeV, μ_0=M_H
Normalized 7pt scale uncertainty
1.3
1.2
1.1
1.0
0.9
0.8
0.7
5
10
50
100
500
1000
5000
M_H(GeV)
$\hat{\sigma}_{N3LO}$, MSHT20 aN3LO
$\hat{\sigma}_{N3LO}$, NNPDF4.0 aN3LO
0.5($\hat{\sigma}_{N2LO}$+$\hat{\sigma}_{N3LO}$), CT18Z NNLO, N3LO scale dep.
NNLO vs. partial N3LO

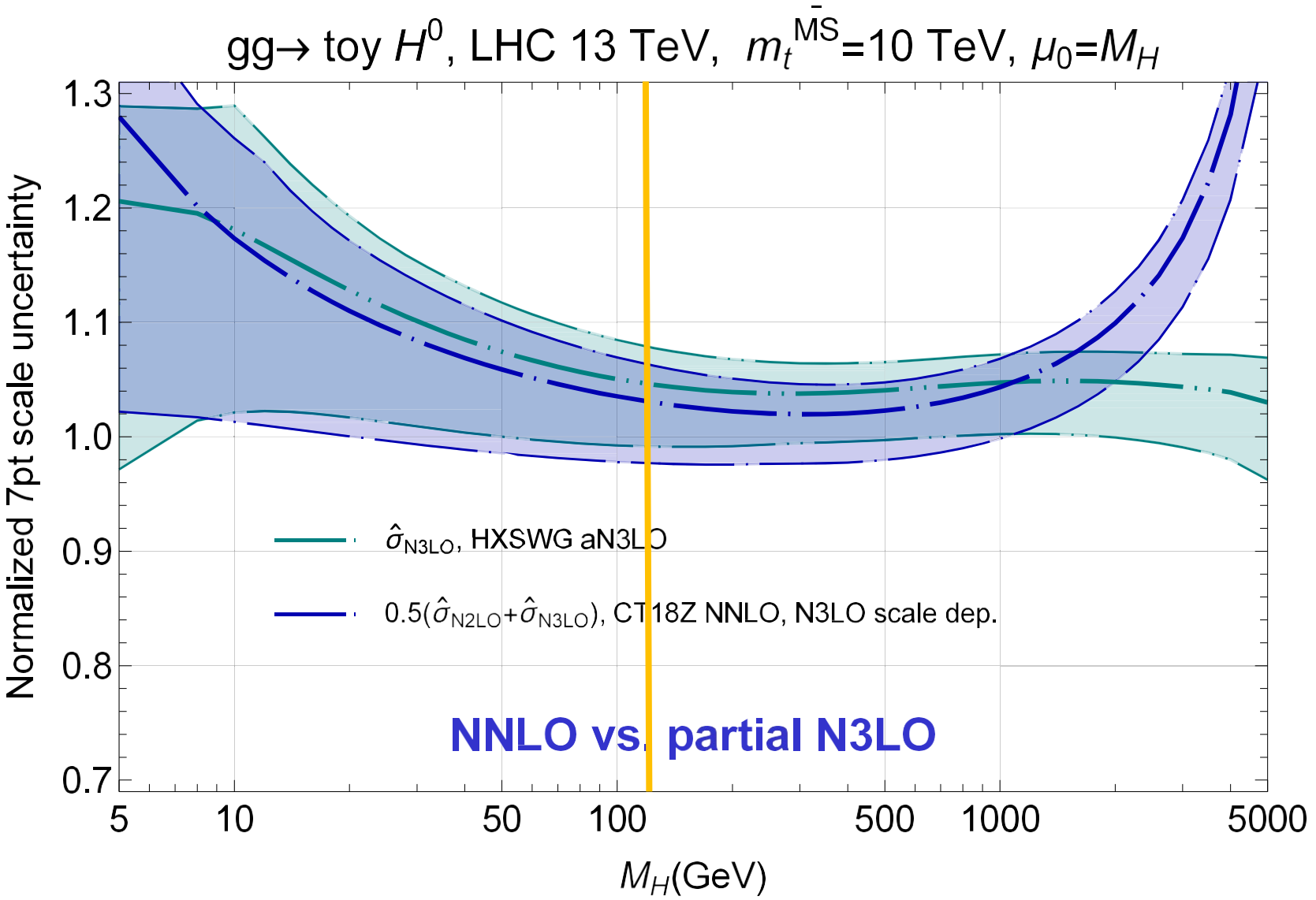

The aN3LO corrections reproduce well the shape of the CT18Z gluon PDF obtained at NNLO with a saturation-inspired factorization scale in DIS, also consistently with BFKL-resumed NNPDF and xFitter NNLO PDFs

The CT18 NNLO+ prescription agrees with the combined HXSWG prescription everywhere except at $M_H > 1.5$ TeV ($x > 0.1$), where tensions between the earlier and newer data sets introduce some differences; added LHC jet/$t\bar{t}$ data reduce this difference in the CT25 fit (2408.04020)

$pp \to Z'X$, central scales $\mu_{F0} = \mu_{R0} = M_{Z'}$

[More figures in the supplemental .pdf file]

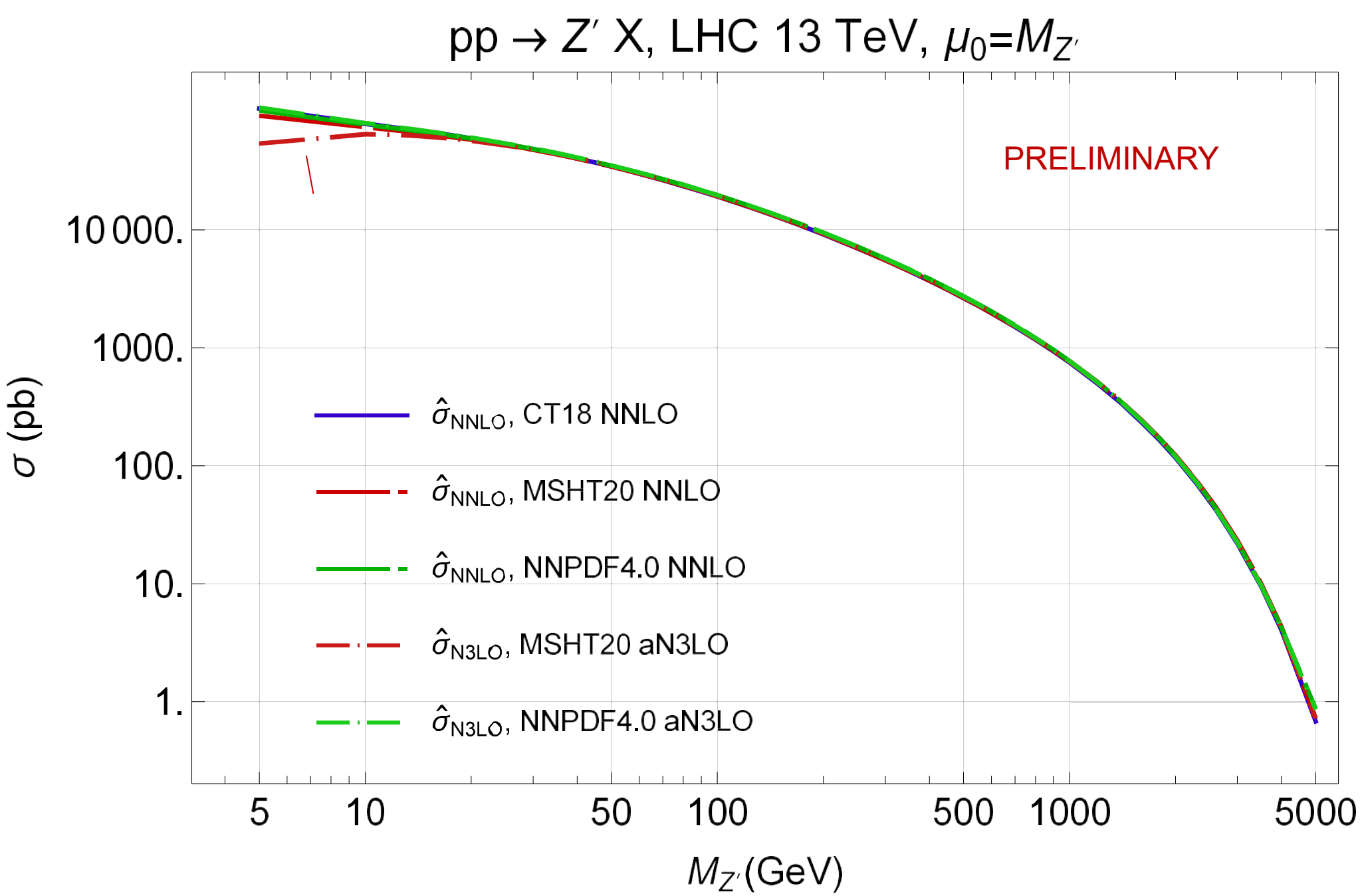
pp → Z′ X, LHC 13 TeV, μ0=MZ′
PRELIMINARY
σ (pb)
10 000.
1000.
100.
10.
1.
$\hat{\sigma}_{NNLO}$, CT18 NNLO
$\hat{\sigma}_{NNLO}$, MSHT20 NNLO
$\hat{\sigma}_{NNLO}$, NNPDF4.0 NNLO
$\hat{\sigma}_{N3LO}$, MSHT20 aN3LO
$\hat{\sigma}_{N3LO}$, NNPDF4.0 aN3LO
5
10
50
100
500
1000
5000
MZ′(GeV)

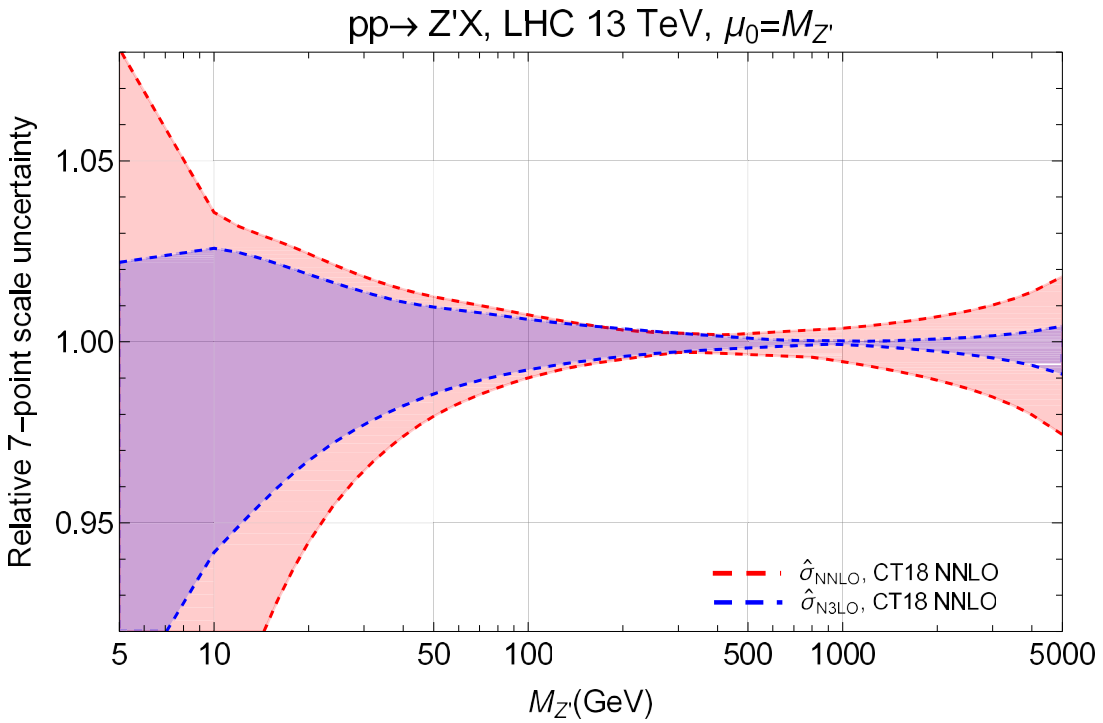

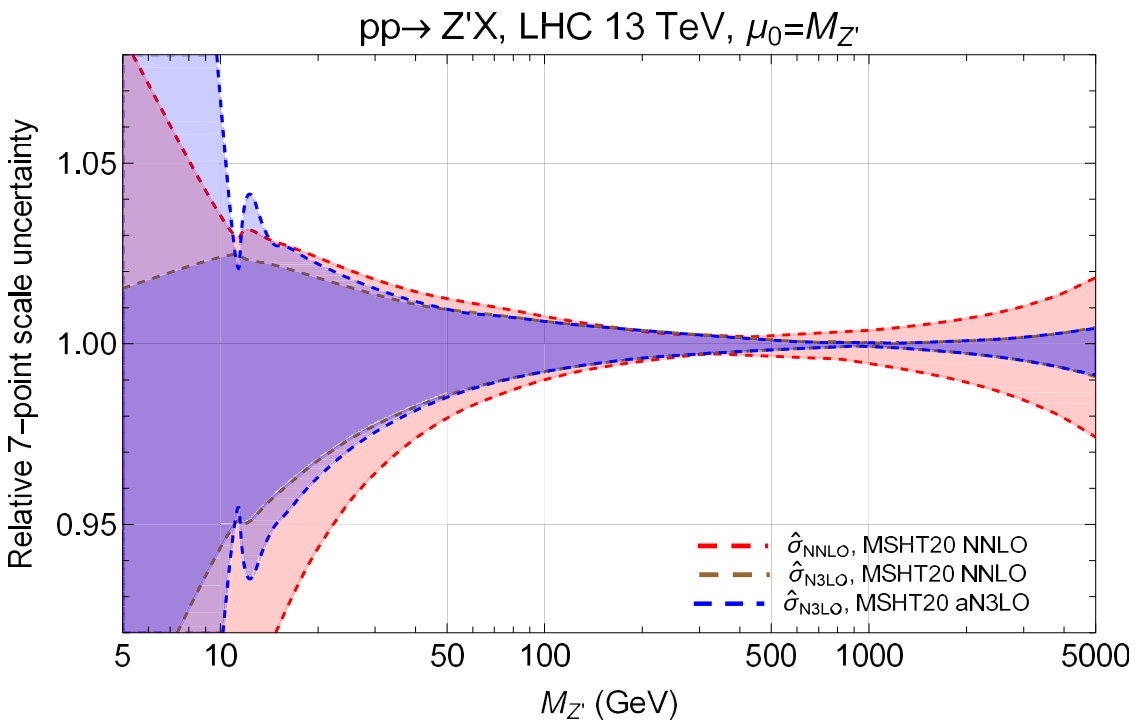

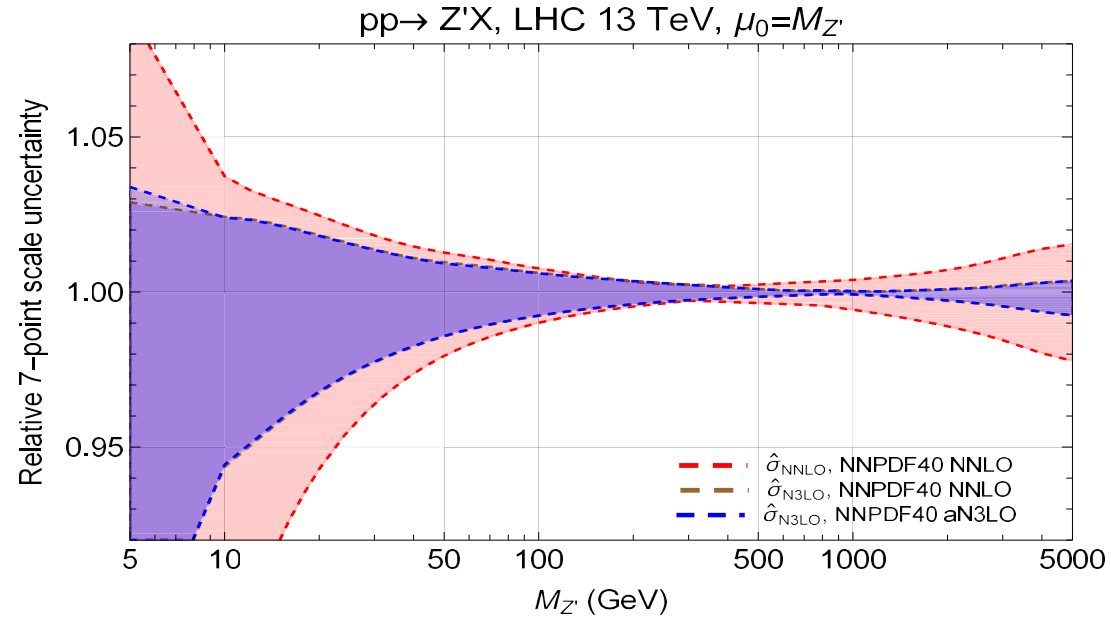

Notice the scale on the y-axis: uncertainties are smaller than in the $gg \to HX$ case

N3LO scale uncertainty is about the same with either NNLO or aN3LO PDFs

b-quark threshold effects at 10 GeV

NNLO+ vs NNLO

CTEQ-TEA “NNLO+” correction is similar to the two aN3LO ones

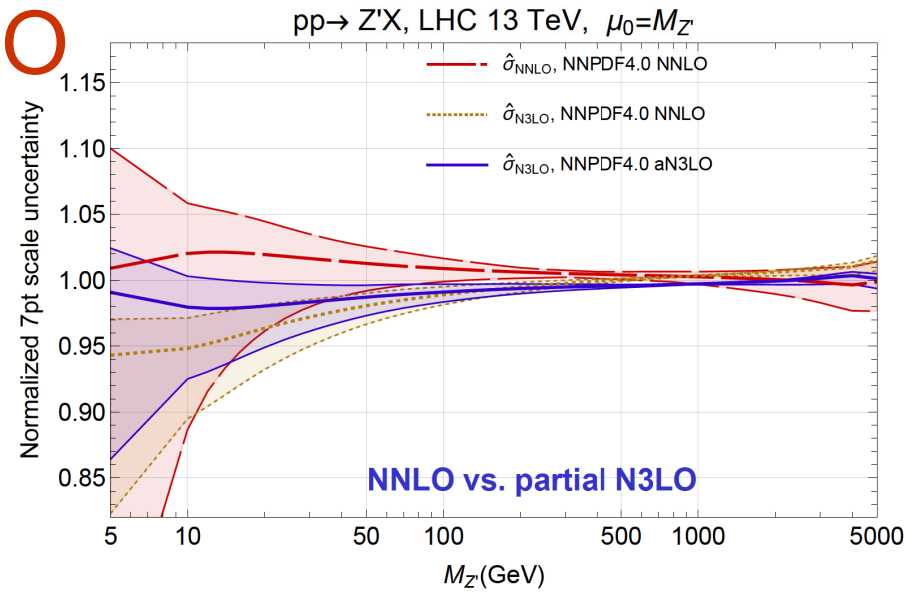

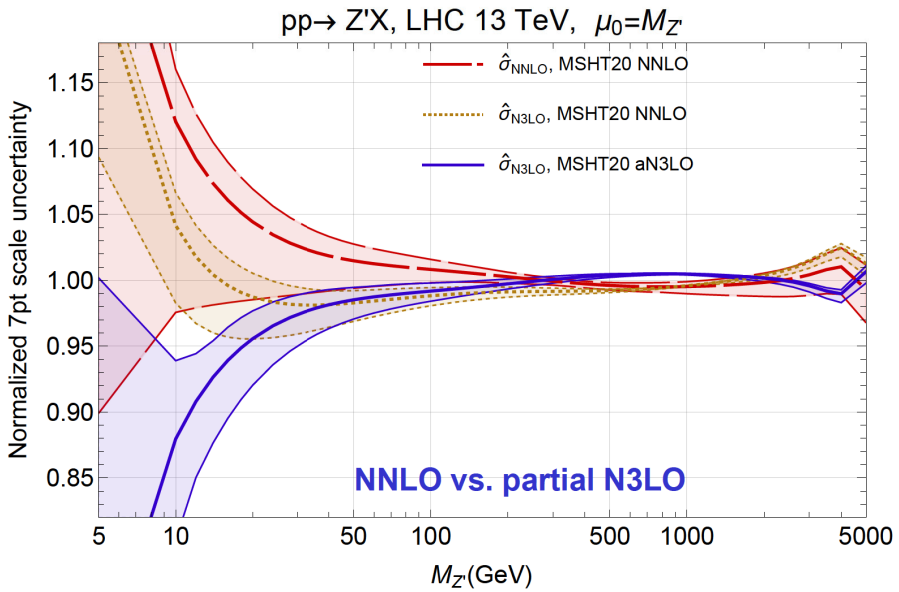

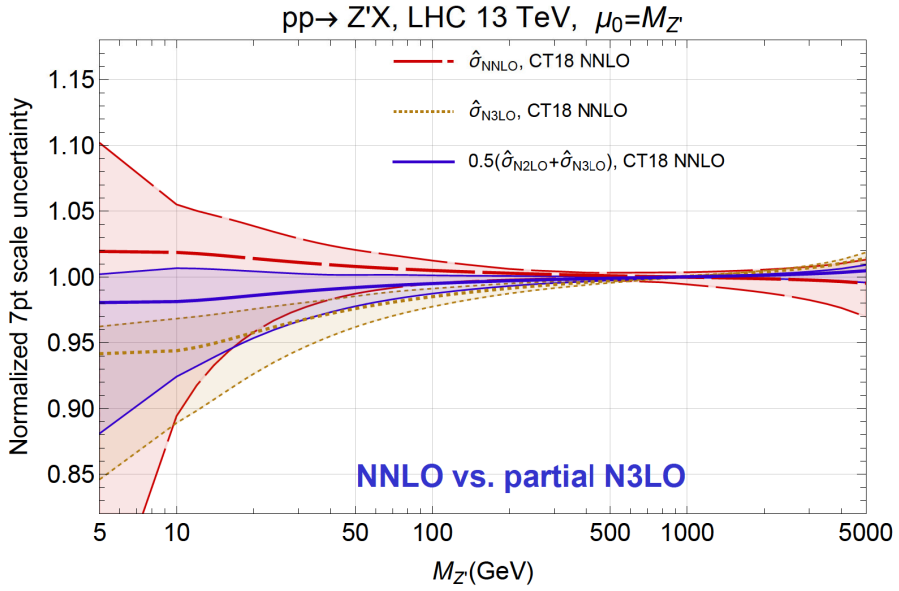

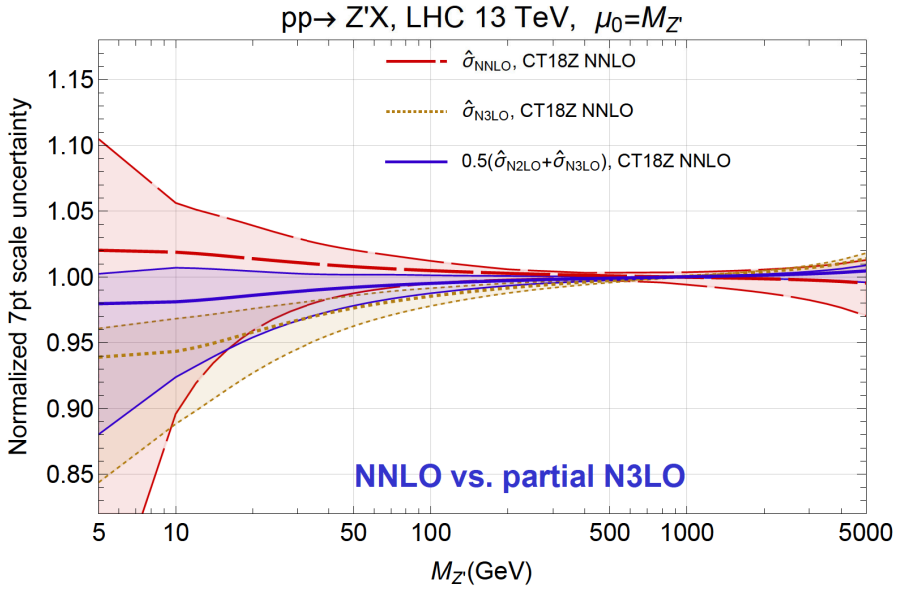

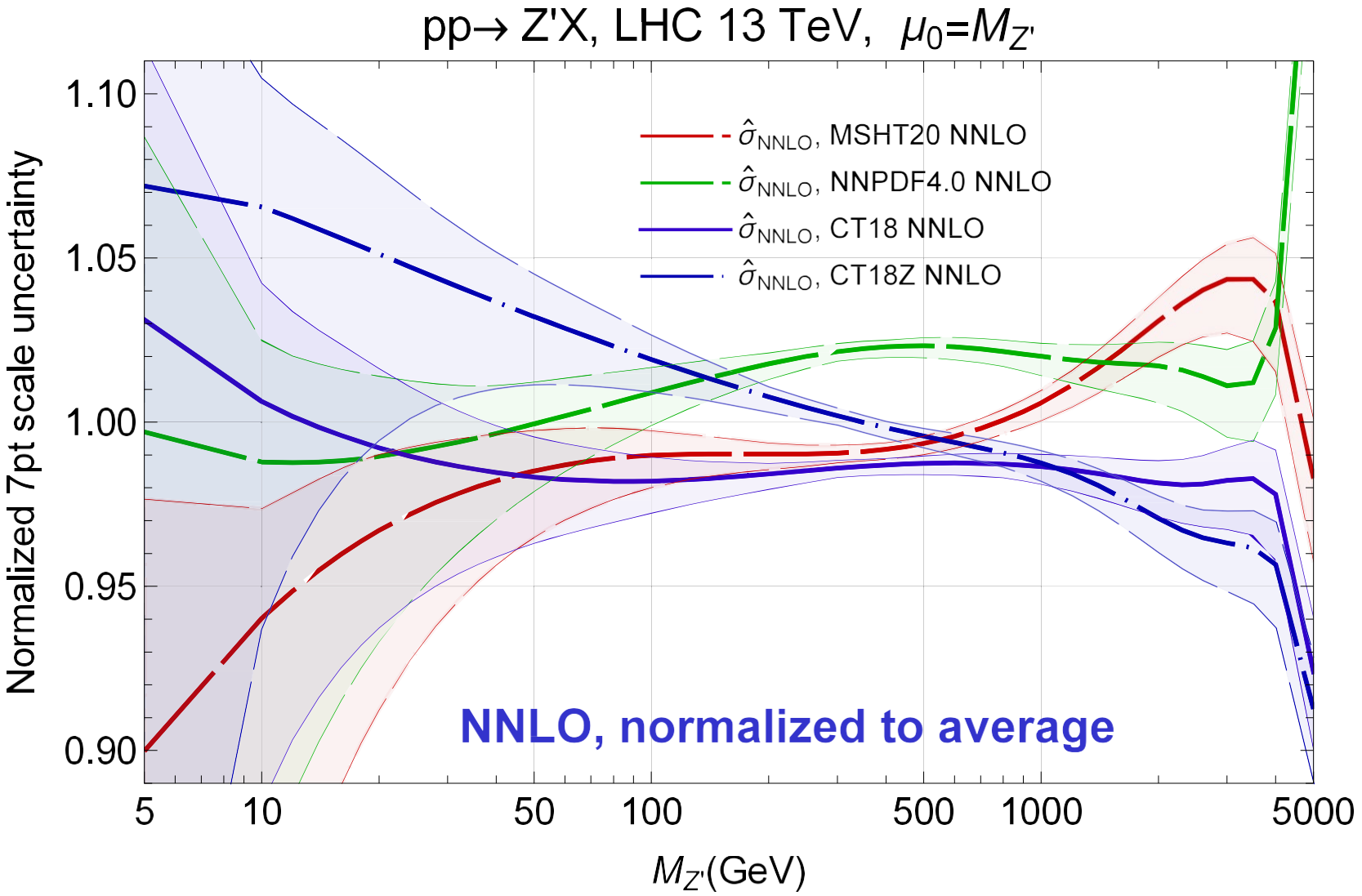
pp→ Z'X, LHC 13 TeV, $\mu_0=M_{Z'}$
Normalized 7pt scale uncertainty
1.10
1.05
1.00
0.95
0.90
$\hat{\sigma}_{NNLO}$, MSHT20 NNLO
$\hat{\sigma}_{NNLO}$, NNPDF4.0 NNLO
$\hat{\sigma}_{NNLO}$, CT18 NNLO
$\hat{\sigma}_{NNLO}$, CT18Z NNLO
NNLO, normalized to average
5
10
50
100
500
1000
5000
$M_{Z'}$(GeV)

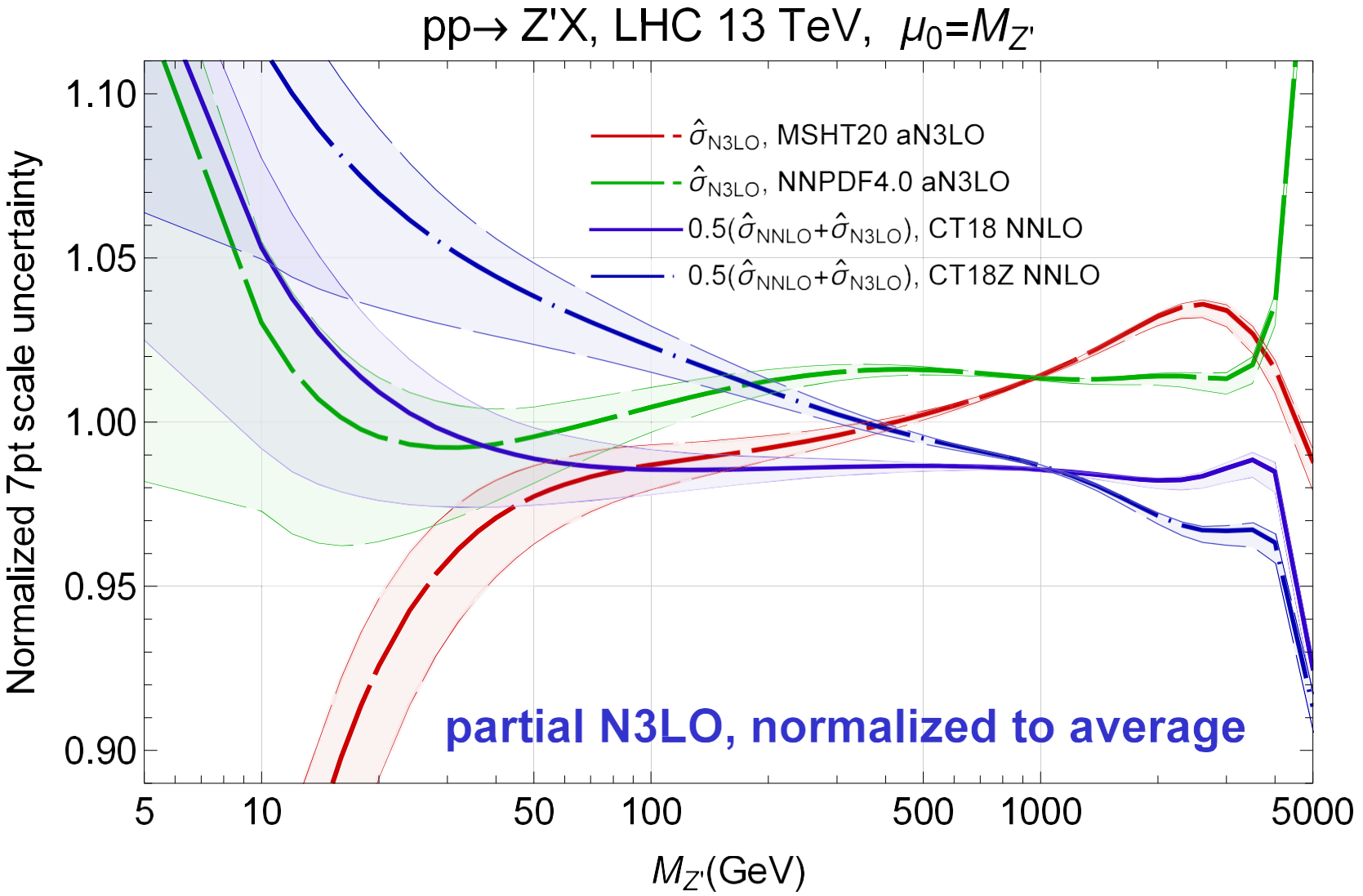

Increased MSHT-NNPDF aN3LO mismatch at $M_Z' < 50$ GeV

Good agreement among the groups at 50-500 GeV

Persistent differences at $M_{Z'} > 1$ TeV, possibly to be reduced with new data

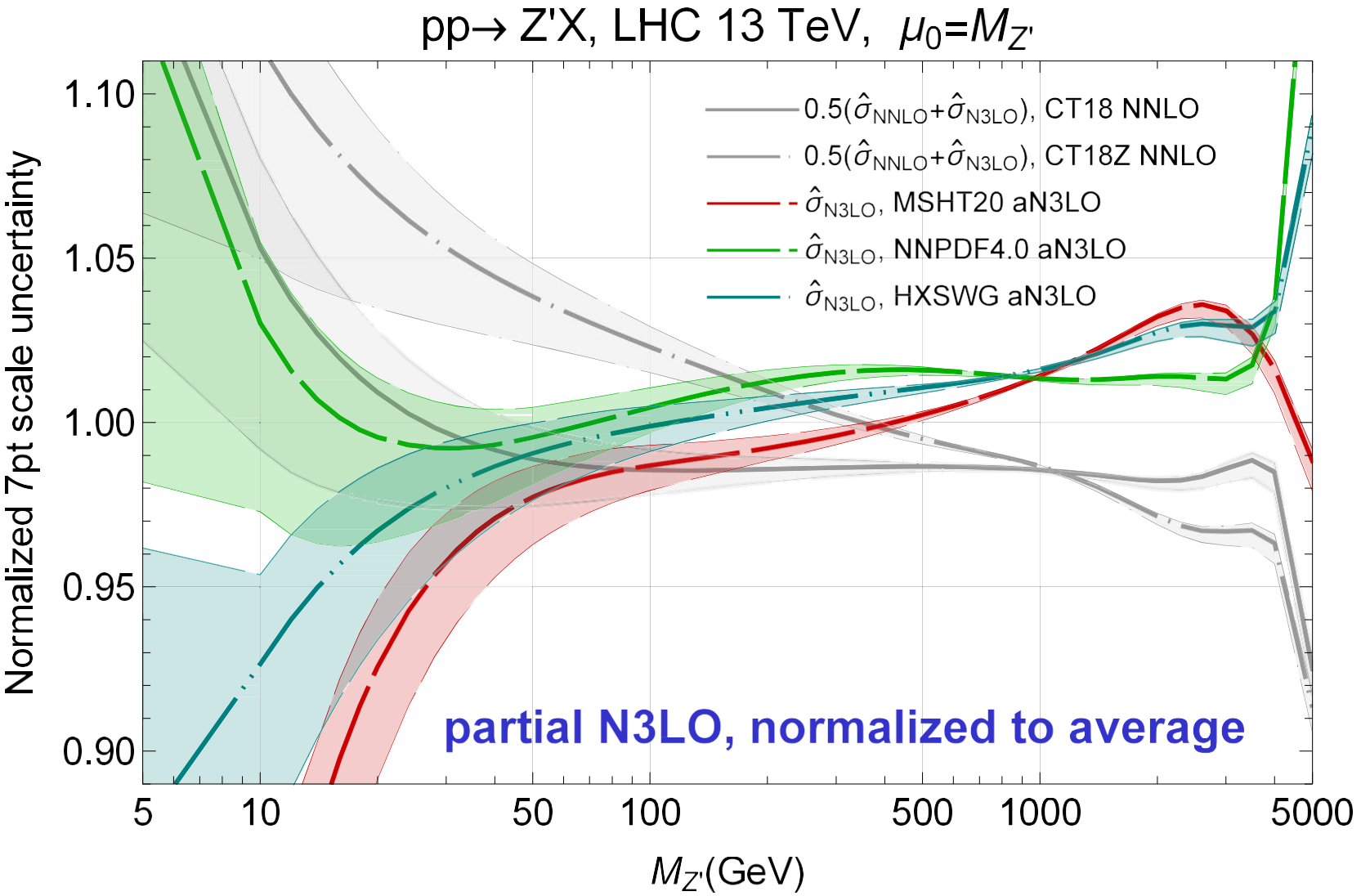

The HXSWG aN3LO combination…

- performs best for 50-500 GeV;
- in agreement with CT18Z NNLO+ at these masses;
- at other $M_{Z'}$, does not capture the full range of NNLO and NNLO+ predictions

NNLO or NNLO+?

Sustained progress by all groups in including N3LO contributions in the PDF fits.

N3LO contributions are still incomplete. Cross section comparisons are not conclusive about superiority of any single NNLO+ technique. The described CT18 NNLO+ and HXSWG aN3LO prescriptions perform similarly for $gg \to H^0$ total cross sections, while these prescriptions capture a part of the variability in the $q\bar{q} \to Z'$ cross sections.

None of the NNLO+ techniques is reliable before thorough benchmarking is performed. A suitable time for such benchmarking is after the imminent implementation of N3LO HQ DIS cross sections in all global fits around 2025.

Many other PDF uncertainties are larger than the N3LO-NNLO differences. Among these, the uncertainties due to the choice of the PDF priors and modeling of systematics affect all global fits and do not automatically decrease at NNLO+. Accounting for them is central for replicability. See, e.g., Courtoy et al., 2205.10444.

THANK YOU FOR YOUR ATTENTION!

Bézier curve

Bézier curves are convenient for interpolating discrete data

The interpolation through Bézier curves is unique if the polynomial degree= (# points-1), there's a closed-form solution to the problem,

$$\mathcal{B}^{(n)}(x) = \sum_{l=0}^{n} c_l \; B_{n,l}(x)$$

with the Bernstein pol.

$$B_{n,l}(x) \equiv \binom{l}{n} x^l (1-x)^{n-l}.$$

The Bézier curve can be expressed as a product of matrices:

- $\underline{T}$ is the vector of x^l
- $\underline{\underline{M}}$ is the matrix of binomial coefficients
- $\underline{C}$ is the vector of Bézier coefficient, c_l, to be determined

$$\mathcal{B} = \underline{T} \cdot \underline{\underline{M}} \cdot \underline{C}$$

We can evaluate the Bézier curve at chosen **control points**, to get a vector of $\mathcal{B} \rightarrow \underline{P}$

$\underline{\underline{T}}$ is now a matrix of x^l expressed at the control points.

$$\underline{P} = \underline{\underline{T}} \cdot \underline{\underline{M}} \cdot \underline{C}$$

Slide by A. Courtoy

Bézier-curve methodology for global analyses — toy model

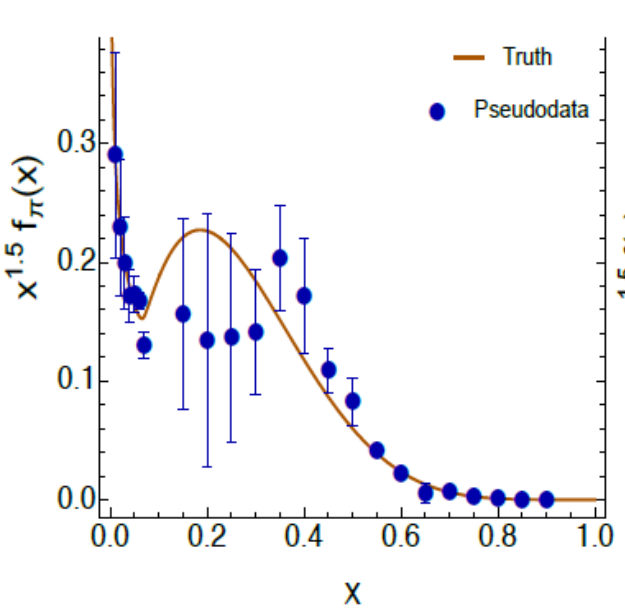

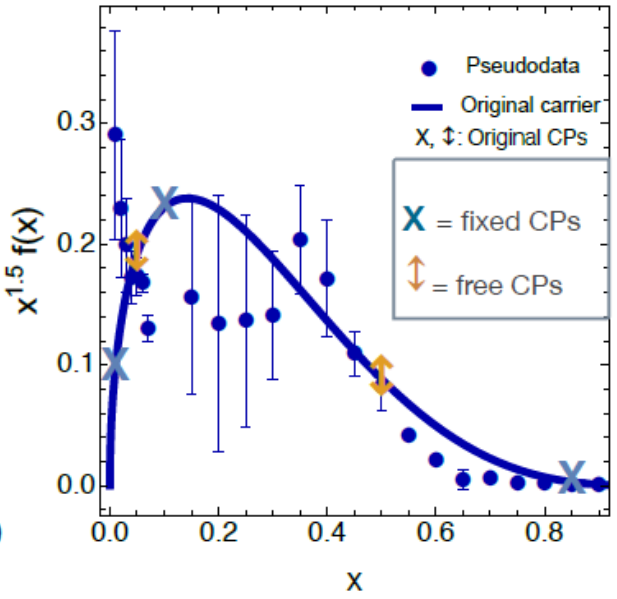

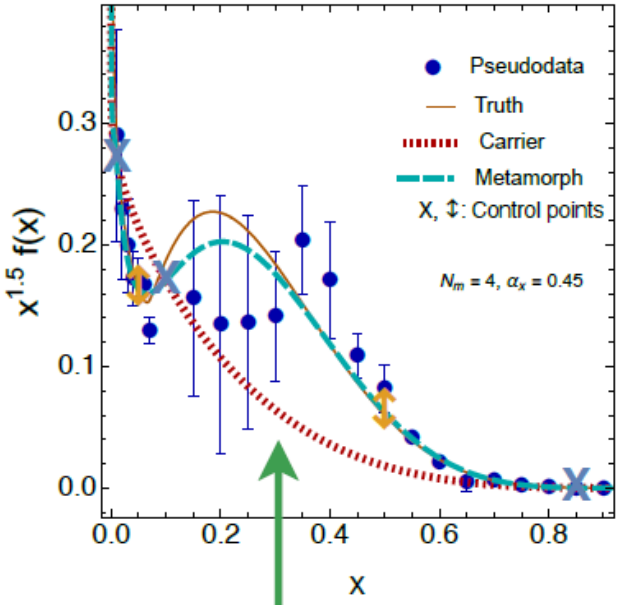

metamorph fit:

$$x\,q(x,Q_0^2) = A'_q\, x^{B_q}(1-x)^{C_q} \times \left(1 + \mathcal{B}^{(N_m)}(x^{\alpha_x}, Q_0^2; \underline{v})\right)$$

with N_m= # CPs-1 for a square-matrices system.

Shift of the control points ($\delta D_q, \ldots$) replace free parameters

N_m= degree of polynomial can vary

δB_q & δC_q allow the carrier to vary

α_x can vary

Slide by A. Courtoy

Bézier-curve methodology for global analyses — toy model

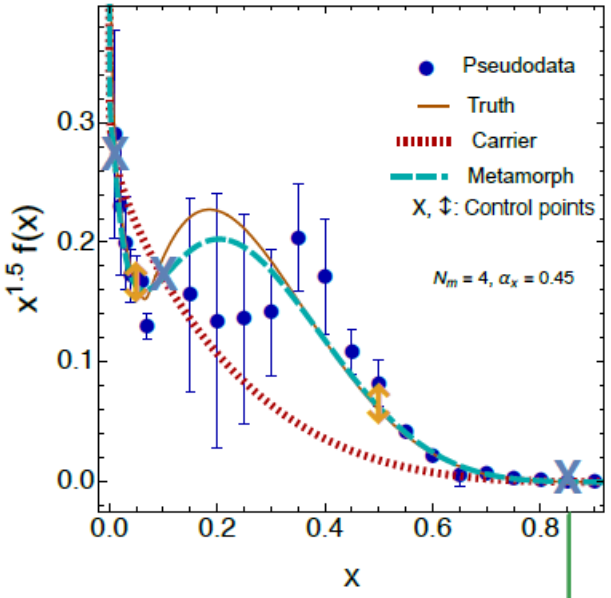

if bootstrapped

sampling on the distribution of data uncertainties

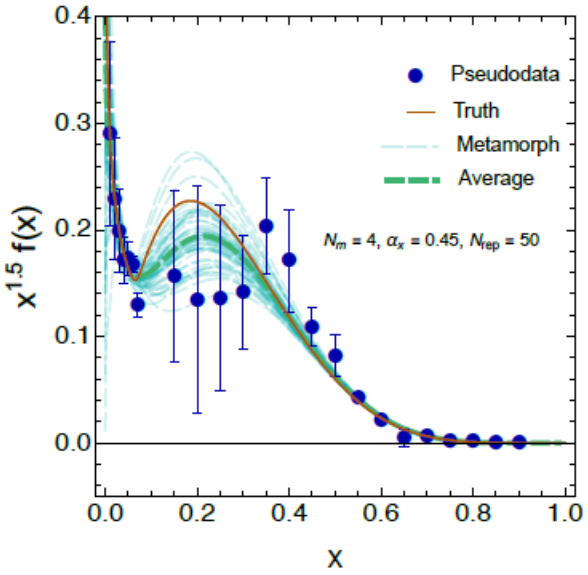

if sampled over `metamorph` settings

sampling over parametrizations

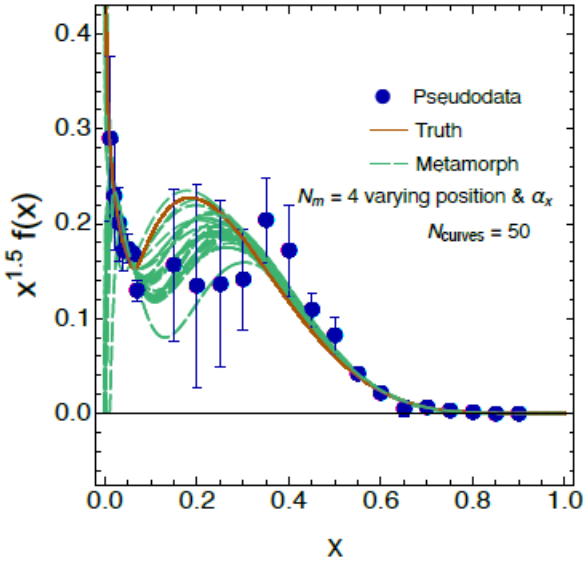

Both samplings can be done in the same analysis, they are not mutually exclusive.

Slide by A. Courtoy